

3. EXPERIMENTAL PROCEDURES

3.1 MATERIALS AND FABRICATION

3.1.1 MATERIALS

Type B edible gelatin with given Bloom strength of 200 and a mesh size of 30 was obtained from Milligan and Higgins Inc. (Jamestown, NY). Resorcinol was obtained from Fisher Scientific Company (Springfield, NJ). Glyoxal, 40% solution in water, was obtained from Aldrich Chemical Company (Milwaukee, WI).

3.1.2 FORMULATION VARIATIONS

Initial formulation of the adhesives was conducted using available literature on gelatin resorcinol formaldehyde (GRF) tissue adhesives as a guide. The three to one weight ratio of gelatin to resorcinol mentioned in the literature was maintained⁴⁻⁷ and formulations with appropriate amounts of water and glyoxal were created that had adequate viscosity and gelation (setting) time. Elastomeric adhesives with qualities such as high initial tack, low viscosity prior to setting, and relatively short setting time, characteristic of good adhesives, were found regardless of the variation of water and glyoxal content by formulation. This large window of adhesive formulations with good adhesive qualities led to the need to understand the material properties of the adhesives as a function of formulation. Three resin formulations were prepared according to Table 3.1. The amount of water for formulation W was increased compared to control formulation C while the amount of glyoxal was decreased slightly. The amount of glyoxal was increased for formulation G compared to control formulations C.

Table 3.1.1 Weight fractions for three different GR-DIAL formulations

Formulation C	weight %	formulation W	weight %	formulation G	weight %
Gelatin	30	gelatin	21	gelatin	23
Resorcinol	10	resorcinol	7	resorcinol	8
Water	56	water	68	water	56
Glyoxal	5	glyoxal	3	glyoxal	14

3.1.3 FABRICATION METHODS

Samples were fabricated by mixing a 3:1 ratio of gelatin to resorcinol with the appropriate amount of deionized water by formulation. The mixture is heated and stirred at 45⁰C using a stirring hotplate and magnetic stir bar until a homogeneous solution is obtained. The stir bar is removed and the corresponding amount of glyoxal is quickly and thoroughly mixed in by hand using a glass stirring rod. The resin is cast into silicone rubber sample molds, just prior to gelation, then covered, and allowed to set for an hour, Figure 3.1.1. The covered molds are then frozen to improve handling of the material, and then stored in airtight containers to prevent aging.

Two different types of molds were used for production of samples. Block samples were produced from a mold that yielded multiple samples with dimensions of 5 mm in depth, 13 mm in length, and 4 mm in height, Figure 3.1.2. A sheet mold was utilized for the remaining samples that were fabricated, and from the sheet molds appropriate specimens could be sectioned with uniform thickness. For mechanical testing, the frozen sheet of material was removed from the mold and placed between sheets of wax paper. Dog bone shaped samples were punched from the sheet material using a Dewes and Gumbs Die Inc. (Long Island City, NY) manual expulsion press. The press is fitted with an ASTM standard D638 metric reduced die having measurements shown in Figure 3.1.3. The thickness of the dog bone samples were approximately 2 mm depending on the cast sheet thickness. Once the samples have been removed from the mold and appropriately punched or sectioned, the samples were frozen again until use. A maximum of 48 hours was allowed between the casting and testing process to minimize any possible water loss or aging that may occur.

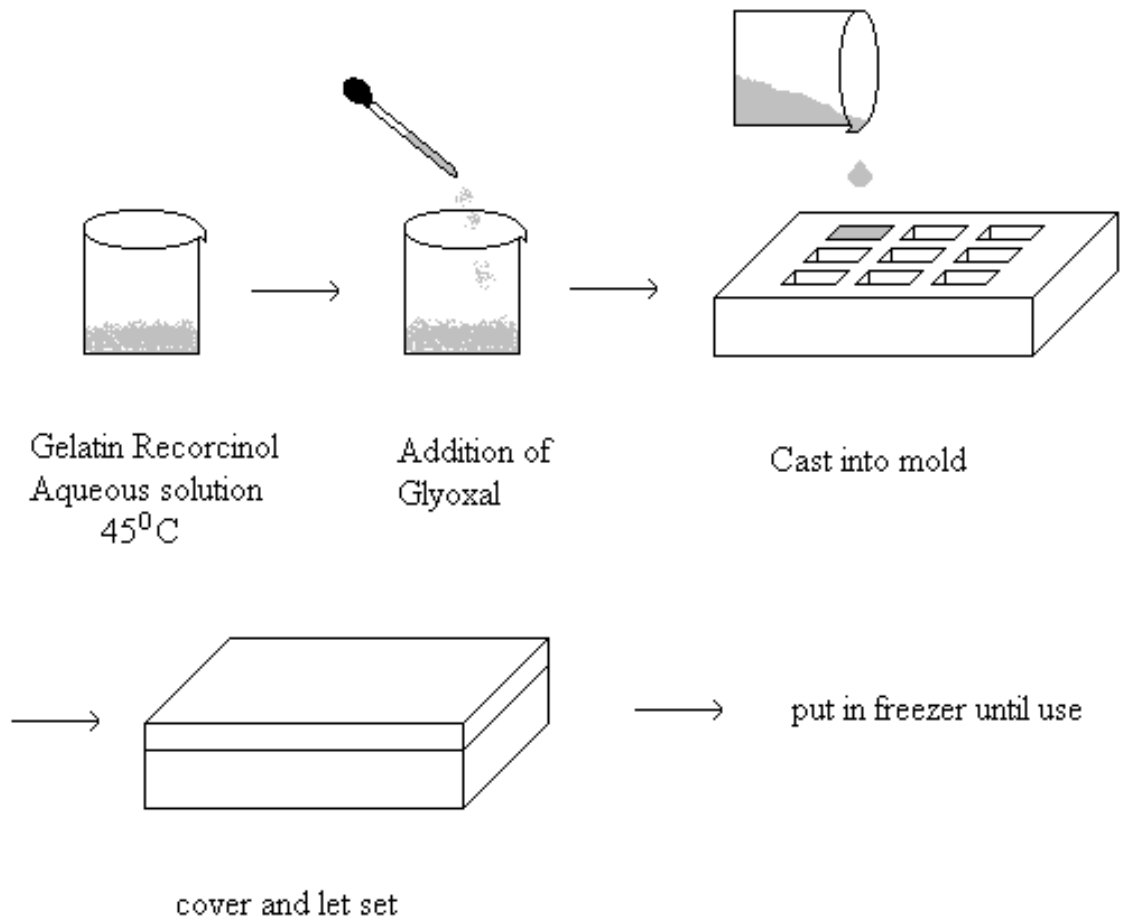


Figure 3.1.1 Fabrication procedure for experimental samples

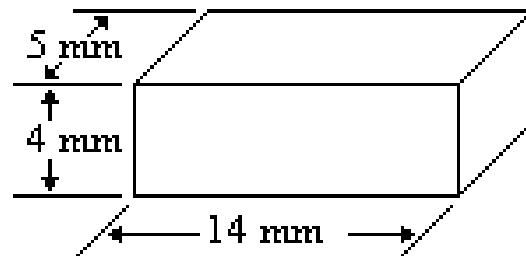


Figure 3.1.2. Illustration of block samples fabricated for experiments

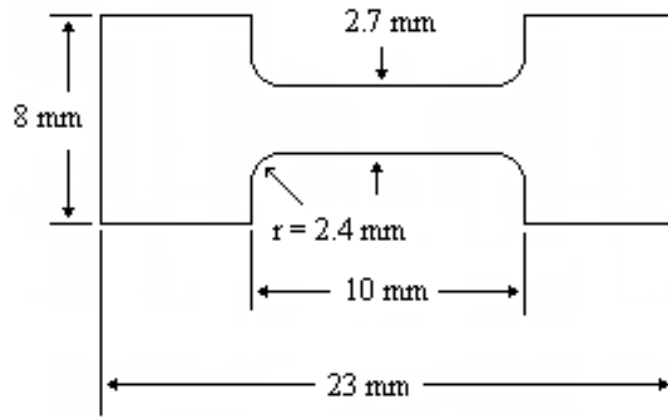


Figure 3.1.3. Illustration of dog bone test specimens

3.2. OBSERVATIONS DURING FABRICATION

3.2.1 pH MEASUREMENTS

Measurements of pH were conducted to determine if the pH of the mixture before and after cross-linking of each formulation varied significantly, since the viscosity, gelation rate, and reaction with glyoxal may be affected. The pH of the resin was measured using a digital handheld 315 pH/Ion meter (Corning Inc., Corning, NY) with accuracy of ± 0.05 pH. The pH meter was calibrated using pH 7 and pH 4 buffer solutions. The pH was measured using three batches of each formulation, with measurements taken prior to and after gelation. The pH measurement of the water used was 6.13.

3.2.2 GELATION TIME

Measurements of gelation time were conducted to determine the amount of time available before solidification as well as the possible dependence on pH and gelatin concentration by formulation. For gelation time tests, six batches of each formulation were prepared identically in 250 ml beakers containing identical amounts of gelatin and resorcinol. Corresponding amounts of water and glyoxal were added to each beaker according to formulation. Each beaker was heated to 45 °C prior to addition of glyoxal. Identical stir bars weighing 7.25 g were used for each test and a stir setting of 1 on the same stirring hot plate was used. Gelation time was measured by the time period required for the magnetic stirring bar to stop stirring following addition of glyoxal. The method used was similar to the measurement method for gelation time mentioned in the literature.²³⁻²⁵

3.3 ABSORPTION/DESORPTION

3.3.1. SWELLING MEASUREMENTS

Swelling of the adhesives was conducted to evaluate the degree of swelling by formulation. Three block samples of each formulation were completely immersed in 50 ml each of deionized water at room temperature. The mass uptake of water was recorded utilizing a Mettler AE 50 digital balance (Highstown, NJ) with accuracy of ± 0.1 mg. The original mass of each sample was recorded prior to immersion. Measurements of the mass were taken thereafter over a period of two days. The excess water was removed carefully from samples using paper towels. The time between measurements increased as the time progressed (i.e., 10 minutes, 30 minutes, 60 minutes, 2 hours, 3 hours, 5 hours etc.), until equilibrium was reached.

3.3.2 DRYING MEASUREMENTS

Drying of adhesive samples was conducted to evaluate the degree of water loss from the samples in an oven at 37°C over a period of two to three days. Five rectangular samples of each formulation were sectioned from material cast in a sheet mold and utilized. Measurements of the mass were taken using a Mettler AE 50 digital balance (Highstown, NJ) with accuracy of ± 0.1 mg. The initial mass and dimensions of each sample were measured prior to placing the samples in an oven at 37°C . The remaining mass measurements were taken over a period of two to three days with the time between measurements increasing as time progressed (i.e., 10 minutes, 30 minutes, 60 minutes, 2 hours, 3 hours, 5 hours etc.), until equilibrium was reached.

3.4 THERMAL ANALYSIS

Thermal analysis was conducted to evaluate the glass transition temperature and characterize the phase behavior of water in the adhesives.

3.4.1 DYNAMIC MECHANICAL SPECTROSCOPY

A Perkin Elmer DMA 7 Dynamic Mechanical Analyzer (Norwalk, CT) was used to characterize the glass transition temperature by measuring the storage and loss moduli of the material as a function of temperature. The temperature scale of the instrument was calibrated using pure samples of indium and zinc. Block samples were used for testing of the freshly frozen adhesives. Three samples of each formulation were tested in three point bending mode, Figure 3.4.1, with a span length of 10 mm. A static force of 500 mN and a dynamic force of 417 mN were applied to the samples while the temperature was ramped from -75°C to 15°C at 3°C per minute. The peak in the loss modulus was identified as T_g . Dried specimens to be tested were sectioned from material cast in a sheet mold and subsequently placed in an oven for 19 hours at 37°C . Three samples of each formulation were tested in three-point bend mode using a span length of 5 mm. A smaller span length was used for the dried samples because shrinkage of the samples occurred during the drying process. The dried samples were heated at a temperature rate of 3°C per minute from -50°C to 50°C , applying the same static and dynamic forces as used for the fresh samples. The difference in the temperature ranges for testing between the fresh frozen and dried samples was necessary because the dried samples would be expected to have a higher T_g than the fresh samples.

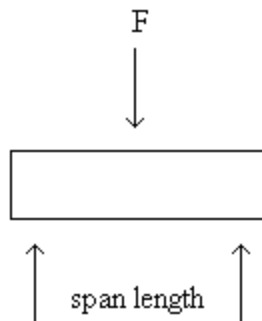


Figure 3.4.1 Illustration of three point bending mode

3.4.2 DIFFERENTIAL SCANNING CALORIMETRY

Differential Scanning Calorimetry (DSC) was conducted to obtain the change in enthalpy of the ice melt for the adhesive samples. A Perkin Elmer Pyris 1 DSC (Norwalk, CT) was utilized. The temperature scale of the instrument was calibrated using pure samples of indium and decane. Both fresh frozen samples and dried samples were tested. Fresh frozen samples were sectioned from material cast in a sheet mold; while dried samples were also sectioned from material cast in a sheet mold, and placed in an oven for 19 hours at 37⁰C prior to DSC testing. The sectioned material samples weighed between 5 and 15 mg and were placed in pre-weighed aluminum sample pans and sealed with lids. Samples were analyzed at a temperature ramp of 3⁰C per minute from -50⁰C to 100⁰C and at 10⁰C per minute from -100⁰C to 200⁰C. A droplet of deionized water was also analyzed at 3⁰C per minute from -50⁰C to 100⁰C to measure the change in enthalpy of the ice melt for pure water.

3.4.3 THERMOGRAVIMETRIC ANALYSIS

Thermogravimetric analysis was conducted on the adhesives using a Perkin Elmer TGA 7 (Norwalk, CT) to evaluate the water loss from the adhesives as a function of temperature. The temperature scale of the instrument was calibrated using pure samples of Perkalloy and Nickel. Prior to testing, the samples were placed in a titanium pan and the initial weight was recorded by the instrument. The samples were heated in an atmosphere of nitrogen at 5⁰C/min from 25⁰C to 400⁰C. Both fresh frozen samples and dried samples were tested. Fresh frozen samples were sectioned from material cast in a sheet mold; while dried samples were also sectioned from material cast in a sheet mold, and placed in an oven for 19 hours at 37⁰C prior to TGA testing.

3.5 MECHANICAL TESTING OF ADHESIVES

3.5.1 TENSILE TESTING

Tensile testing was used to evaluate the elastic modulus and strength of the adhesives. A Texture Expert Texture Analyzer (Scarsdale, NY) screw driven mechanical test frame, equipped with a 50 kg load beam was employed. Dog bone samples of fresh frozen material and material dried for 19 hours in an oven at 37⁰C were utilized for testing. For fresh frozen samples, the specimens were removed from the freezer, the length, width and thickness of each specimen recorded, and the specimens were quickly placed into the grips for testing. The specimens were tested ten minutes after they were placed into the grips, which allowed for the specimens to equilibrate to room temperature. Since placing and keeping the material in the grips was quite difficult, fiberglass screen wire was used to prevent the specimens from slipping in the grips. The fresh frozen specimens had variable thickness with an average of 1.76 ± 0.21 mm. Dog bone specimens that were dried for 19 hours at 37⁰C had variable thickness with an average of 1.13 ± 0.26 mm. Specimens were loaded at 0.3 mm/sec, corresponding to a true strain rate of 2.25/min, which is a relatively low strain rate. The modulus, tensile strength and strain at failure were analyzed using Microcal Origin 5.0 software (Microcal Software Inc., Nothampton, MA).

3.5.2 STRESS RELAXATION

Stress relaxation testing was conducted on fresh frozen samples to evaluate the visco-elastic behavior of the adhesives. Dog bone specimens identical to those used for tensile testing were used for stress relaxation tests. The Texture Expert Texture Analyzer was employed for Stress Relaxation testing, using tensile grips. Prior to installing the samples in the grips, each sample was removed from the freezer and the dimensions were measured. After installing each sample into the grips, ten minutes time lapsed before stress relaxation testing to allow each sample to equilibrate to room temperature. Fiberglass screen wire was utilized again to prevent slippage of the samples from the grips. The thickness of the samples varied with an average of 2.14 ± 0.47 mm. Samples were loaded at 10mm/s to approximately 270% strain and held, while the load decay of each sample was recorded over a period of 1000 seconds or approximately 17 minutes each.

3.6 ADHESIVE TESTING

3.6.1 LAP SHEAR TESTING OF ADHESIVE BONDED GLASS SUBSTRATES

Lap shear strength testing was conducted on adhesive formulations bonded to glass slide adherends. The samples were made using two glass slides (25.4 mm wide, 76.2 mm in length, and 1 mm thick). Prior to application of the adhesive, the glass slides were washed with soap and hot water and wiped with ethanol. The glass slides were set on a level surface and bonded with the adhesive on matching surfaces of the glass slides having an area of 645 mm² (1in.²), with bond thickness of approximately of 1 mm, Figure 3.6.1. The samples were allowed to set for approximately one hour prior to testing. A set of fresh frozen samples and samples dried at 37⁰C for 19 hours were prepared. Prior to each test the bond thickness and length were measured and the grips were aligned with the adherends to prevent eccentric loading. The specimens were tested at a strain rate of 0.8 mm/s, using ASTM D816 measurement of adhesive strength of rubber cements as a guideline. This ASTM standard was chosen because the adhesives have similar mechanical properties to rubber cement. The dried lap shear specimens were visibly dry on the outer edges of the bond, while the inner portion of the bond remained compliant, Figure 3.6.2. The average shear strength of all tests was found from the peak in the stress measured. The stress concentration on the adhesive joint was analyzed according to Volkersen's equations outlined in section 2.9.4.

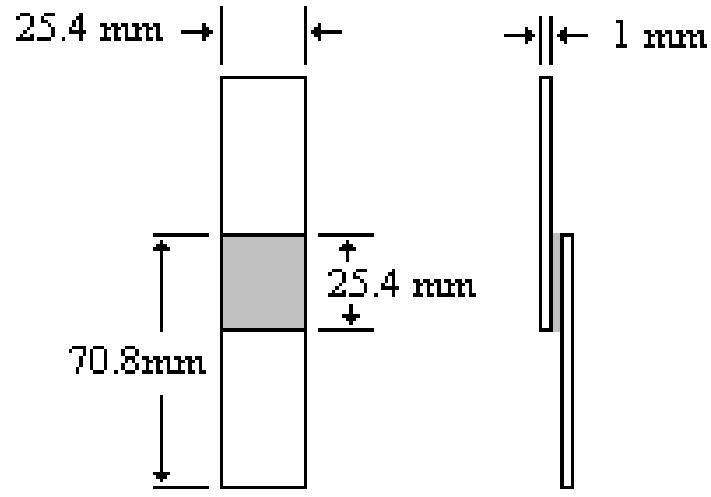


Figure 3.6.1 Illustration of lap shear test specimens

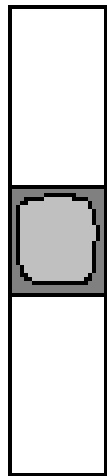


Figure 3.6.2. Illustration of dried lap shear test specimens

3.6.2 LAP SHEAR TESTING OF ADHESIVE BONDED BOVINE TISSUE

Lap shear testing using bovine (cow) skin adherends was conducted on formulation C to compare to the values of adhesive strength found in the literature. Fresh, frozen bovine skin was provided by the Virginia-Maryland Regional College of Veterinary Medicine necropsy lab. The cow skin was prepared by shaving the hair to the best extent possible, removing the excess muscle and connective tissue by means of scalpel, and rinsing the skin of dirt and other residue. The cow skin was cut into strips approximately 1 in. (25.4 mm) wide and 3 in. (76.2 mm) in length. The two dermal sides of the cow skin were bonded together on a level surface with a bond area of approximately 645 mm² (1in.²), and bond thickness of approximately 1.5 mm to 2.0 mm, Figure 3.6.3. Prior to each test, the thickness of the cow skin, and the bond area and thickness were measured. The specimens were tested at a strain rate of 0.8 mm/s, exactly the same as the adhesives bonded to the glass substrate.

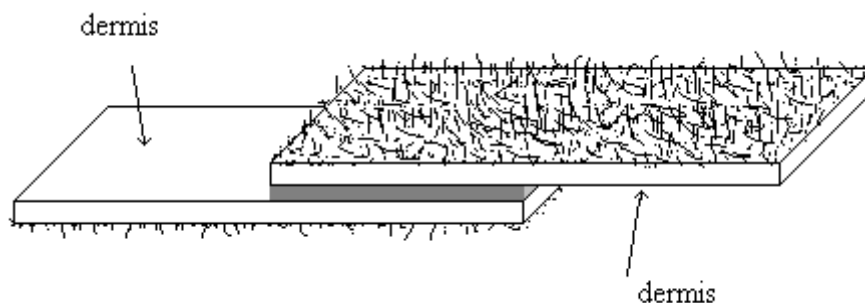


Figure 3.6.3. Illustration of lap shear sample with cow skin adherend

3.7 OPTICAL MICROSCOPY

Optical microscopy was utilized to visually evaluate the bulk adhesive and the glass adherend surfaces of the lap shear specimens. An Olympus BH2-UM optical microscope equipped with an Olympus DP 10 digital camera (Lake Success, NY), and cross polarizers was utilized.

3.8 STATISTICAL ANALYSIS

Statistical analysis was conducted on data having a sample size of three or greater. For all tests, formulations G and W were compared to the Formulation C (control). Student T- tests were conducted using SAS (Cary, NC). Statistical significance was accepted for a p-value less than 0.05. Results are reported as the mean \pm standard deviation.

4. RESULTS AND DISCUSSION

4.1 OBSERVATIONS DURING FABRICATION

4.1.1 pH AND GELATION TIME MEASUREMENTS

There was not a large difference in pH amongst the different formulations before gelation, Table 4.1.1. However, the pH dropped significantly after gelation in the case of formulation G most likely due to the increased amount of glyoxal in the formulation, which is acidic. The measured pH both before and after gelation was within the range of 5.0 to 5.7, which falls roughly in the range of 4.5-5.5 which has been mentioned in the literature as being the minimum for setting time.¹⁰ Judicious addition of salts or other additives have also been mentioned in the literature to be used to control the gelation or setting time.^{5,23-25}

Gelation time measurements for the three formulations of the adhesives are given below in Table 4.1.2. The gelation time was compared to the pH of the solution both before and after gelation, Figure 4.1.1. There appears to be no direct correlation between the pH and gelation time. The gelation time appeared to be dependent on the viscosity of the gelatin solution such that the gelation time increased with decreased gelatin content, Figure 4.1.2. The viscosity was reduced by the addition of both water and glyoxal, therefore the gelation time was most influenced by the gelatin content. The increase in gelation time for formulation W was greater than formulation G that is most likely due to the lower viscosity of water compared to the glyoxal solution. Another consideration that may have affected the gelation time may be that the temperature of the water in the gelatin solution was the same as the gelatin solution (45⁰C) while the glyoxal was at room temperature.

Table 4.1.1 Measurement of pH before and after gelation compared by formulation.

	formulation C	formulation W	formulation G
Before gelation	5.63±0.05	5.66±0.04	5.71±0.03
After gelation	5.31±0.02	5.26±0.05	5.03±0.05*
Average Difference	-0.32±0.06	-0.40±0.02	-0.68±0.04*

* Statistically significantly against formulation C

Table 4.1.2 Gelation time (in seconds) compared by formulation

formulation C	formulation W	formulation G
43±4	176±6*	89±10*

*Statistically significant against formulation C

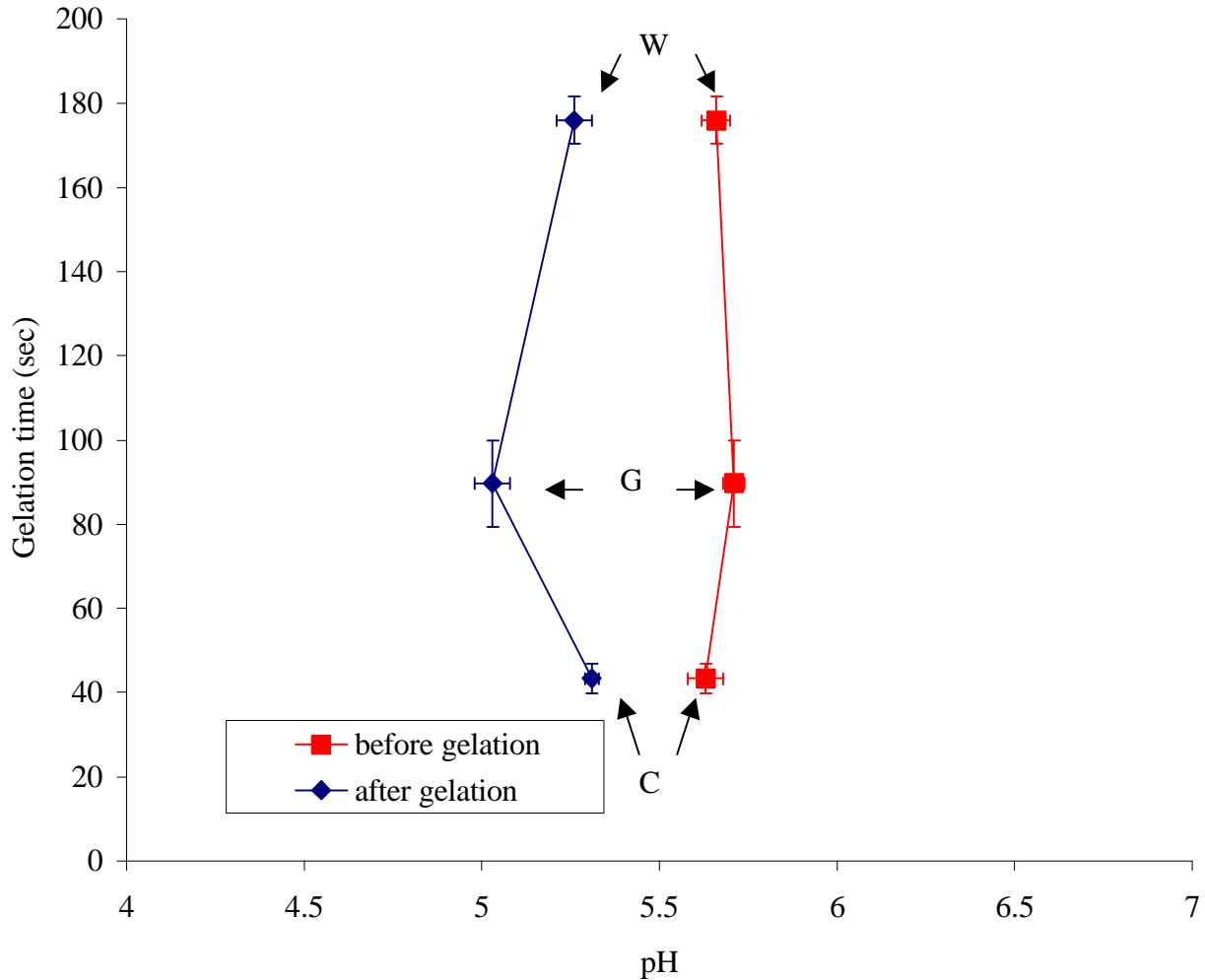


Figure 4.1.1 Graph of gelation time vs. pH measured before and after gelation

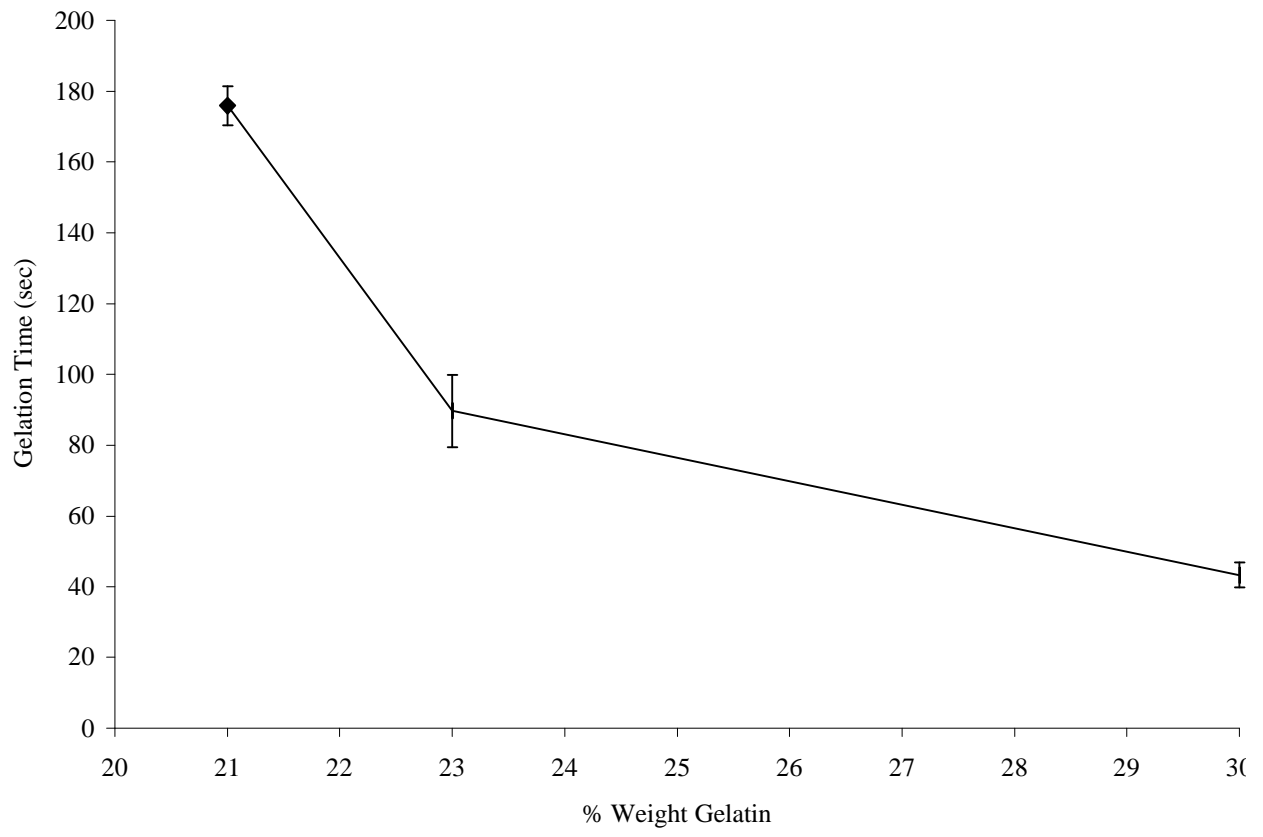


Figure 4.1.2 Graph of gelation time vs. gelatin weight %

4.2 ABSORPTION/DESORPTION

4.2.1 SWELLING MEASUREMENTS

The absorption of water and swelling of the samples with time follows an exponential equation in good agreement with equation 2.5.2. Visually, swelling of the outside edges occurred with the adhesives becoming clear on the outside, while the inner portion of the adhesive appeared as it did initially, being a light yellow color, Figure 4.2.1. The mass uptake of water with time was normalized to the initial mass of each sample prior to immersion for all three formulations and is shown in Figure 4.2.2. The average percent normalized mass uptake of water for each sample is given in Table 4.2.1. A graph of the typical mass measurements with time for swelling experiments fit to equation 2.5.2 are shown in Figure 4.2.3 and the calculated diffusivity of each sample is given in Table 4.2.2. The resistance to swelling of the adhesive formulations was greatly enhanced by addition of cross-linking agent, as noted by the decreased swelling of formulation G compared to formulations W and C. Increased cross-linking content greatly improved the swelling resistance of formulation G as predicted by equation 2.5.3. The equilibrium swelling of formulations W and C were comparable because the content of glyoxal in these formulations was also comparable. However, the swelling of formulations W and C might actually be higher than the reported values since the adhesives became extremely fragile after long time periods of immersion in water. After long periods of time, removing excess water from the adhesives was quite difficult and it was evident that some portions of the adhesive were lost in the process, this was especially evident in the cases of formulation C and W. Perhaps a better method for handling and removing excess water could be devised.

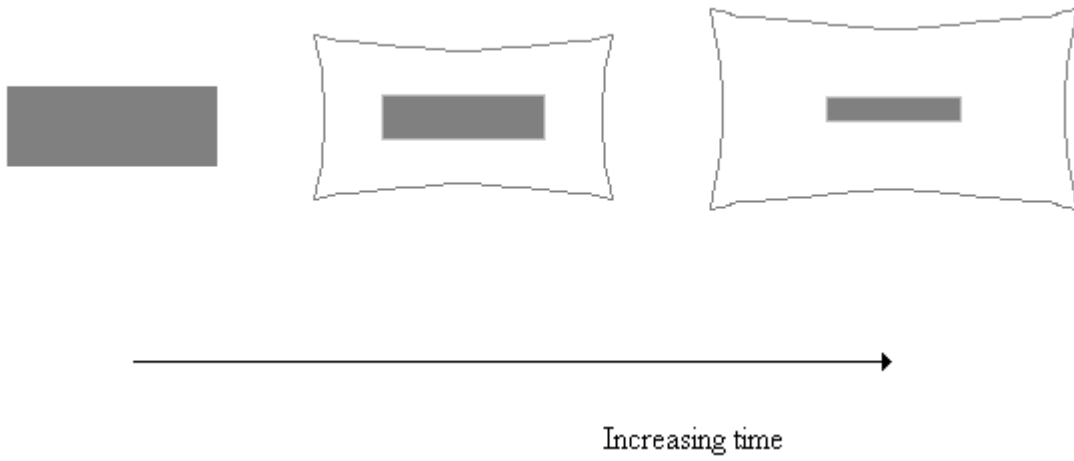


Figure 4.2.1 Illustration of appearance of adhesives with swelling time

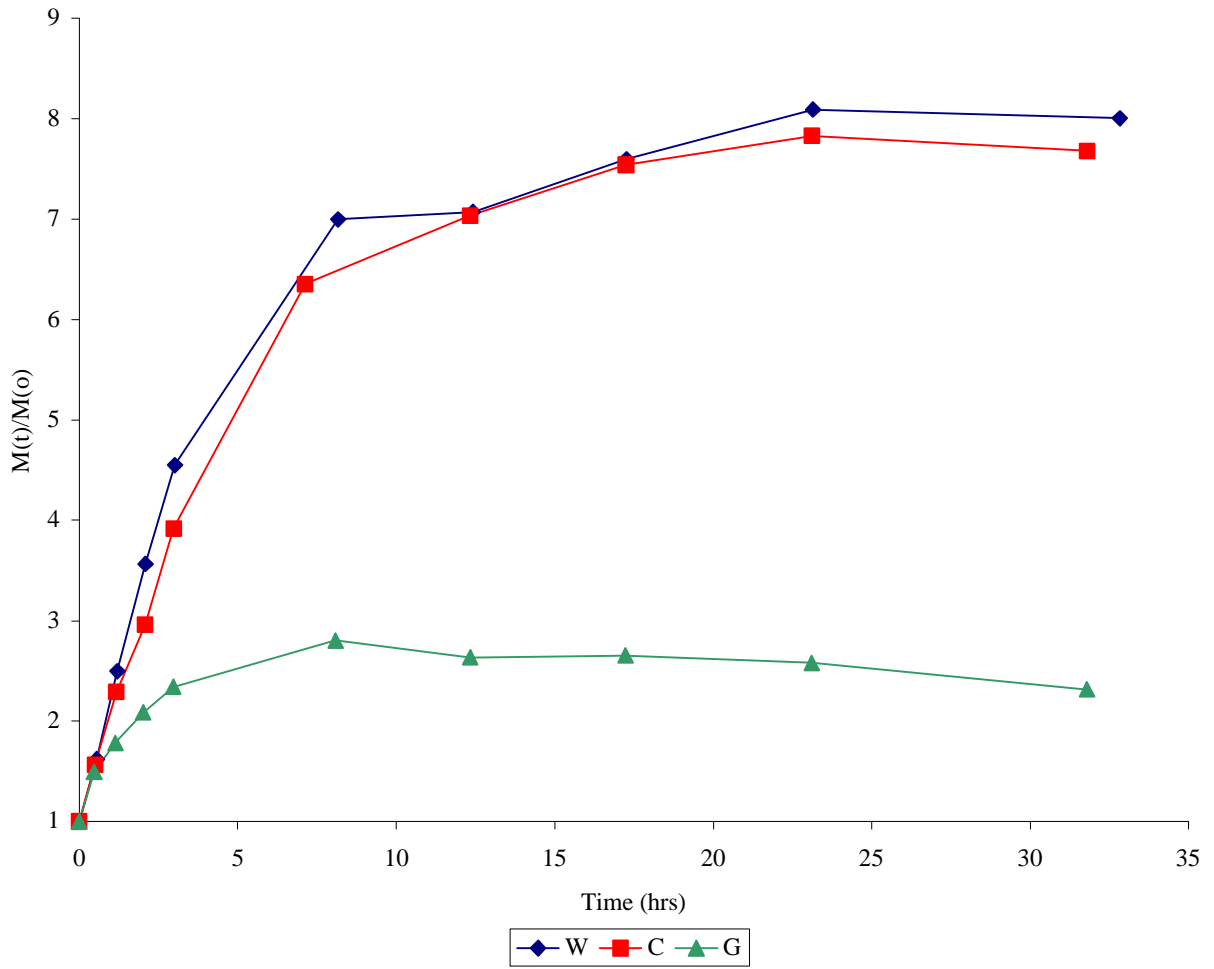


Figure 4.2.2. Typical graph of normalized mass vs. time for water absorption in adhesives

Table 4.2.1 Normalized percent mass uptake at swelling equilibrium by formulation

formulation C	formulation W	formulation G
920%±122	820%±55.6	273%±8.87*

*Statistically significant against formulation C

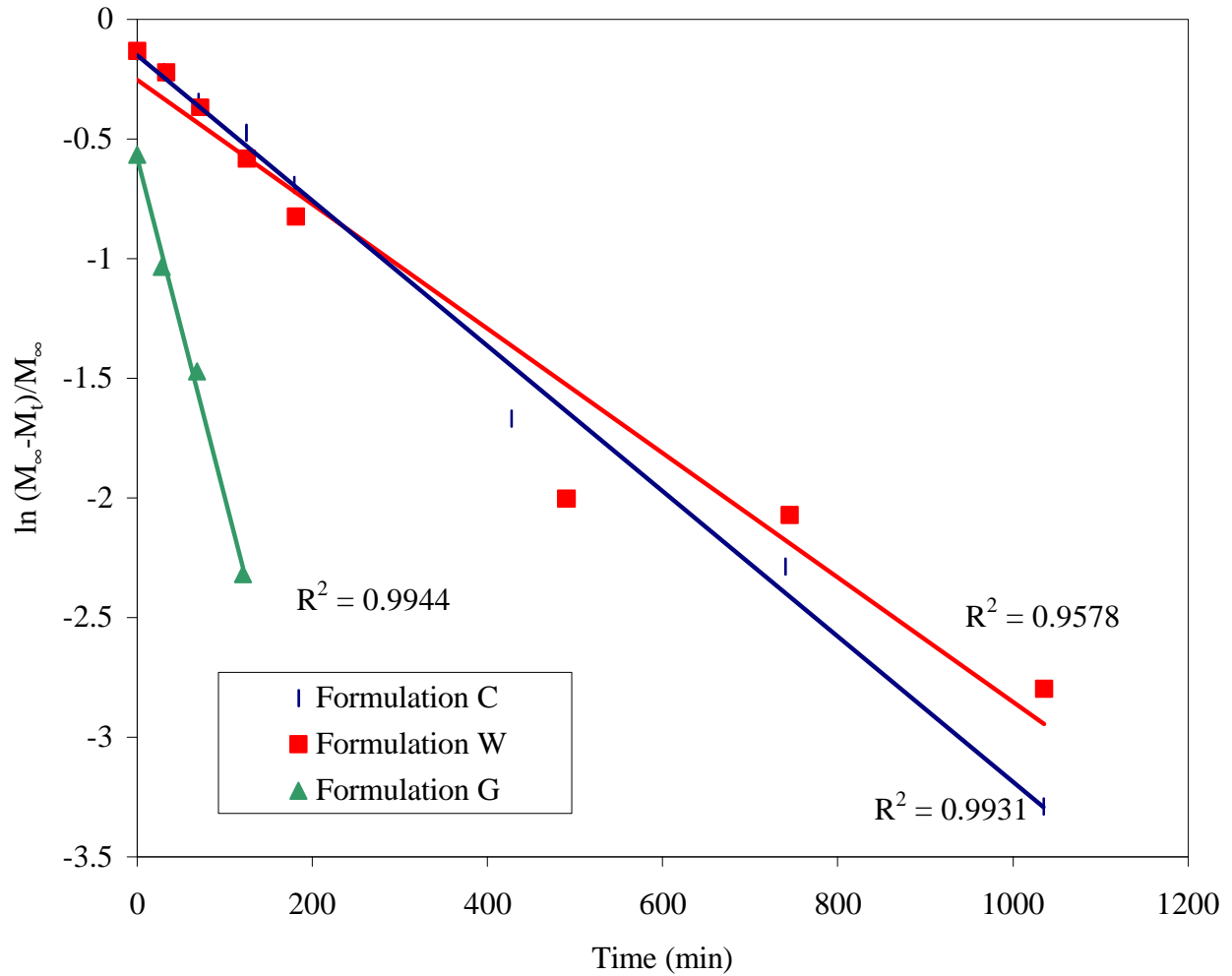


Figure 4.2.3 Graph of typical water absorption measurements fit to equation 2.5.2

Table 4.2.2 Calculated diffusivity of adhesive formulations from swelling experiments

	formulation C	formulation W	formulation G
Diffusivity ($10^{-2} \text{ mm}^2/\text{min}$)	0.75±0.14	0.67±0.052	1.6±0.13*

4.2.2 DRYING MEASUREMENTS

Desorption of water from the adhesives with time resulting from diffusion to the surface and evaporation from this surface follows an exponential equation in good agreement with equation 2.5.2. The water loss from the adhesives also results in shrinkage of the samples. The humidity in the oven ranged from 20% to 60 % relative humidity with the increase due to the water evaporated from the adhesives. The weight loss with time normalized to the weight of each sample prior to placement in the oven of all three formulations is shown in Figure 4.2.4. After about 15 hours, additional weight loss of water from the adhesives was minimal. The water lost from formulation W was much higher compared to formulations C and G, Table 4.2.3. Formulation G, which contains the same amount of water as formulation C, experienced less weight loss compared to formulation C. The weight loss of formulation W was greater than formulation C because it contained more initial water than formulation C. The final weight loss of water of each formulation compared to the original weight content of water and glyoxal in each formulation is shown in Figure 4.2.5. Formulation G, which had initial water content of 56% and glyoxal content of 14%, experienced an average weight loss of 47%, while formulation C also with initial water content of 56% and glyoxal content of 5%, experienced an average weight loss of 51%. Formulation W, which had initial water content of 68% and glyoxal content of 3%, experienced an average weight loss of 65%. In conjunction with results from thermogravimetric analysis (Section 4.3.3), the residual water remaining in the adhesives after infinite time can be assumed to be bound water. The percent residual or bound water can be calculated by subtracting the equilibrium weight loss from the initial water content, and dividing by the initial water content. These results are given in Table 4.2.3. A graph of the typical mass measurements with time for desorption experiments fit to equation 2.5.2 are shown in Figure 4.2.6 and the diffusivity of the adhesive formulations is given in Table 4.2.4.

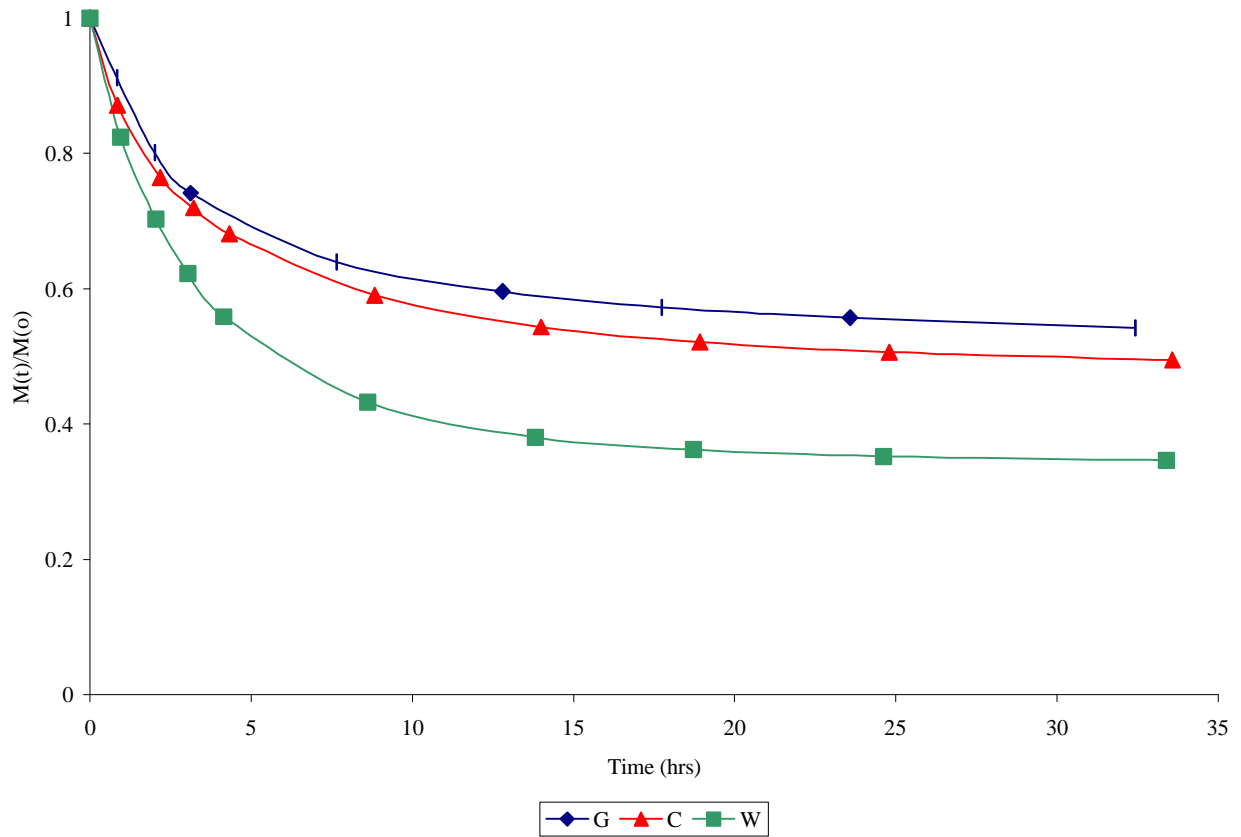


Figure 4.2.4 Typical graph of normalized mass vs. time for water desorption in adhesives

Table 4.2.3 Equilibrium weight loss and percent residual water of dried adhesives

	formulation C	formulation W	formulation G
Equilibrium weight loss %	51.3%±1.3	65.2%±0.1*	46.8%±0.6*
Initial weight % water	56%	68%	56%
% Residual water	8%	4%	16%

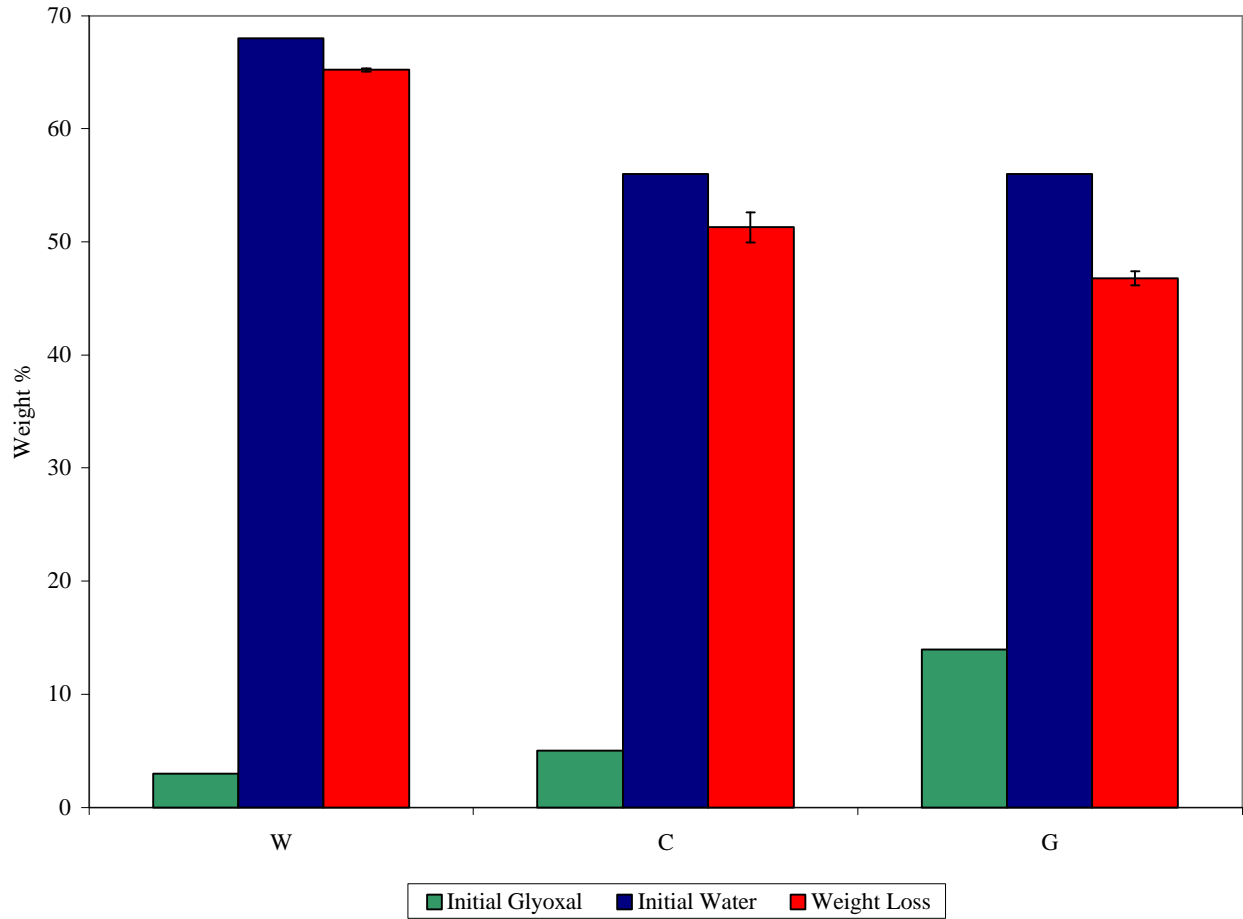


Figure 4.2.5 Graph of initial water and glyoxal content of adhesive formulations compared to weight loss of water due to drying

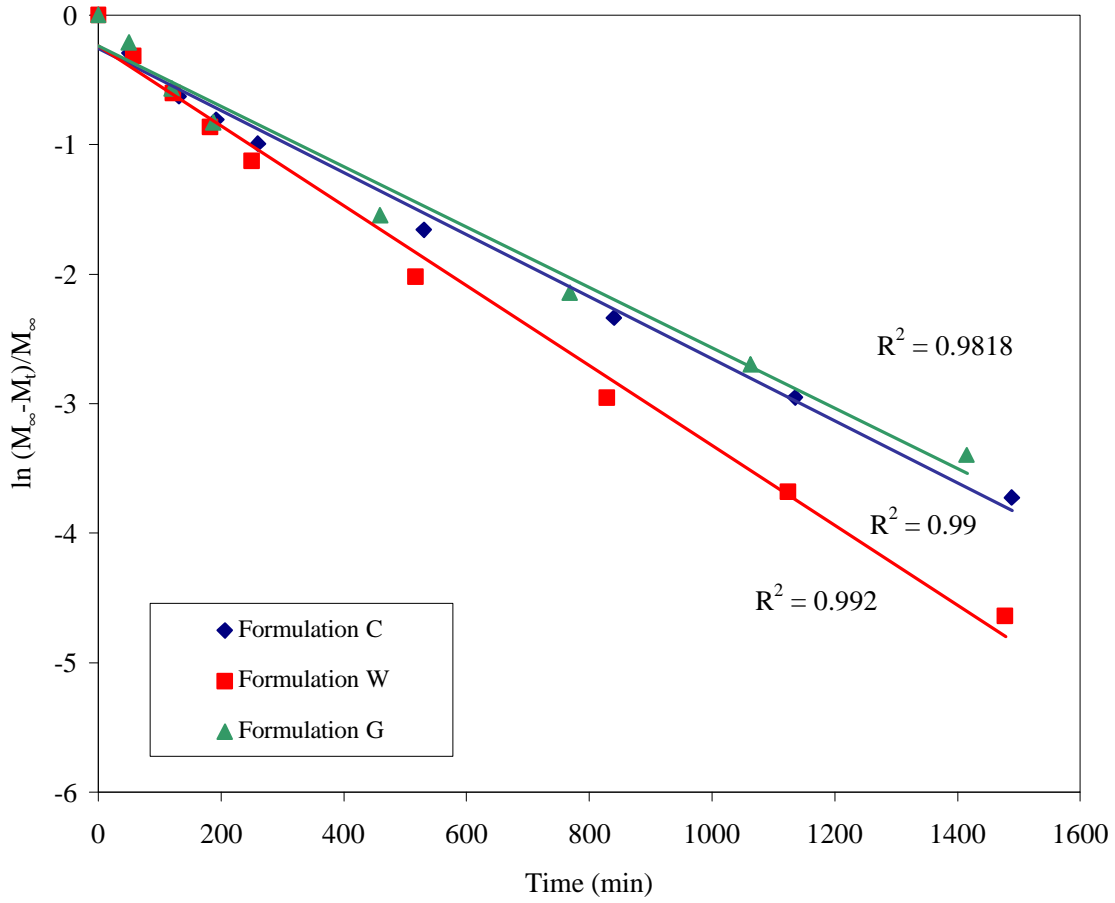


Figure 4.2.6 Graph of typical water desorption measurements fit to equation 2.5.2

Table 4.2.4 Calculated diffusivity of adhesive formulations from drying experiments

	formulation C	formulation W	formulation G
Diffusivity (10^{-2} mm²/min)	3.8±0.27	3.4±0.44	5.2±0.79*

4.3 THERMAL ANALYSIS OF ADHESIVES

4.3.1 DYNAMIC MECHANICAL SPECTROSCOPY

Dynamic Mechanical Spectroscopy (DMS) was conducted on three fresh frozen samples and three dried samples of each formulation. The glass transition temperature was characterized by the maximum in the Loss Modulus, E'' , Figure 4.3.1. The mean \pm S.D. T_g for each formulation is shown in Table 4.3.1. On average, formulation G had the lowest T_g , while formulation W had the highest T_g , though it was not significantly different from formulation C. The glass transition temperature is indirectly proportional to the glyoxal content of the material, where an increase in glyoxal content results in a lower glass transition temperature, see Figure 4.3.2. The depression of the T_g may be a result of the plasticizing effect of bound water in the adhesive, with an increase in bound water resulting from the increase in glyoxal among the formulations. There were no trends observed when comparing the values of the storage and loss modulus of the various formulations of the material below T_g . An increase in storage modulus measured below T_g was expected for formulations with a higher cross-link density, but was not evidenced. DMS was also conducted on samples that were dried for 19-20 hours at 37⁰C for all formulations. The observed T_g values of dried samples are given in Table 4.3.1. The average T_g of formulation G was much lower than for formulations W and C, but the T_g values for formulations C and W were not significantly different. The lower T_g for formulation G may also be a result of an increased proportion of bound water in the adhesive.

The T_g of the adhesives was depressed by the addition of glyoxal, since the glyoxal increased the proportion of bound water to unbound water. It was expected that increased water content in the adhesive systems would act as a plasticizer and depress the T_g but this was not evidenced. The addition of glyoxal caused an increase in the critical concentration of water in the adhesives, causing more water to be bound into the bulk of the adhesive, and to act as a plasticizer. The results for dried adhesives as a function of glyoxal content were conflicting. However, if the T_g was plotted as a function of the percent residual or bound water in the adhesives found from drying experiments, an inverse linear relationship could be seen, Figure 4.3.3.

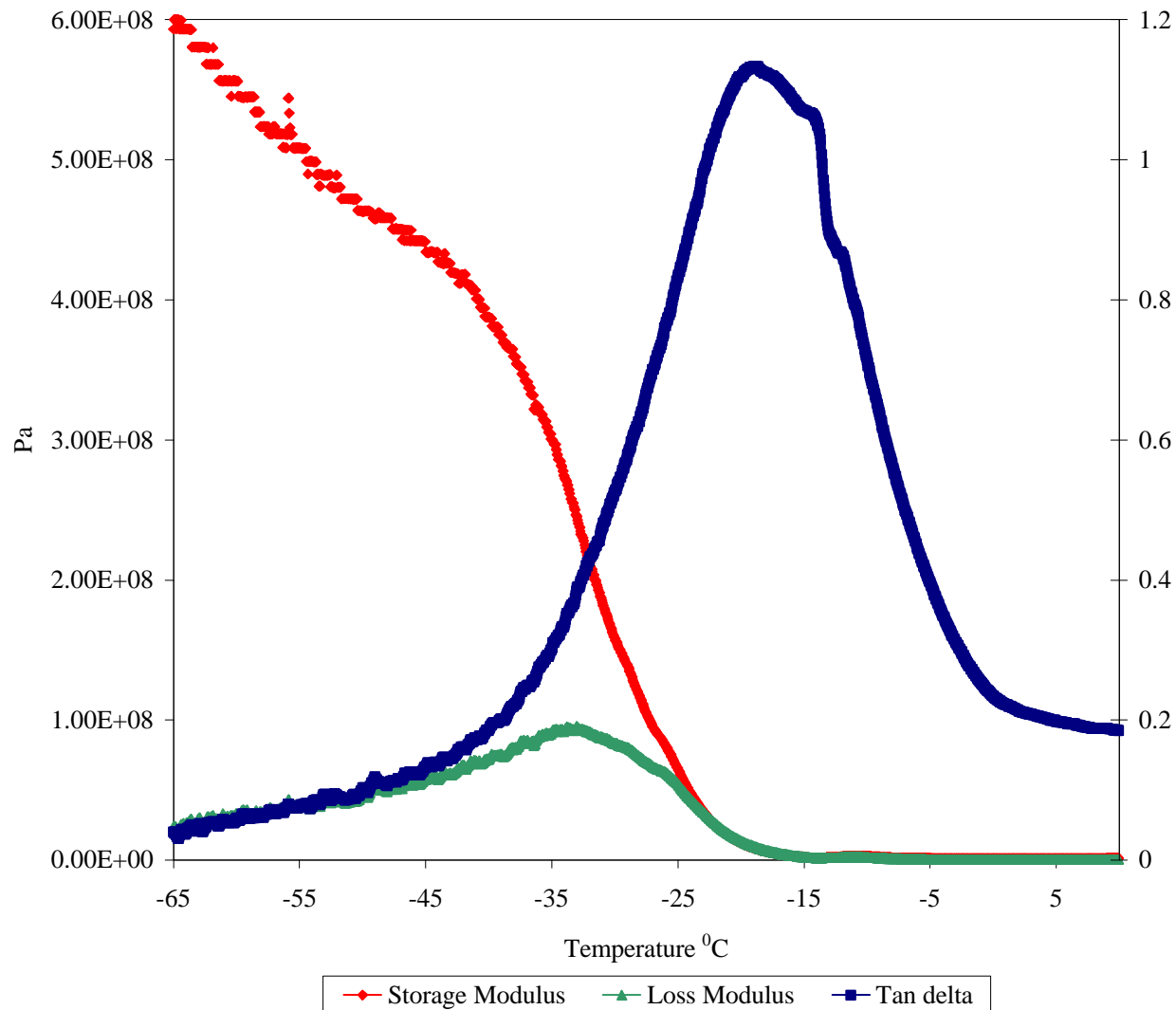


Figure 4.3.1 Typical DMS run for adhesive formulations

Table 4.3.1 Average measured T_g for fresh frozen and dried samples

	formulation C	formulation W	formulation G
Fresh frozen	-17.1±2.9	-14.3±2.8	-34.0±0.9*
Dried	-9.2±1.2	-11.9±2.0	-20.2±2.1*
Average difference	+8.0±2.2	+2.3±2.4	+13.8±1.6

* Statistically significant against formulation C

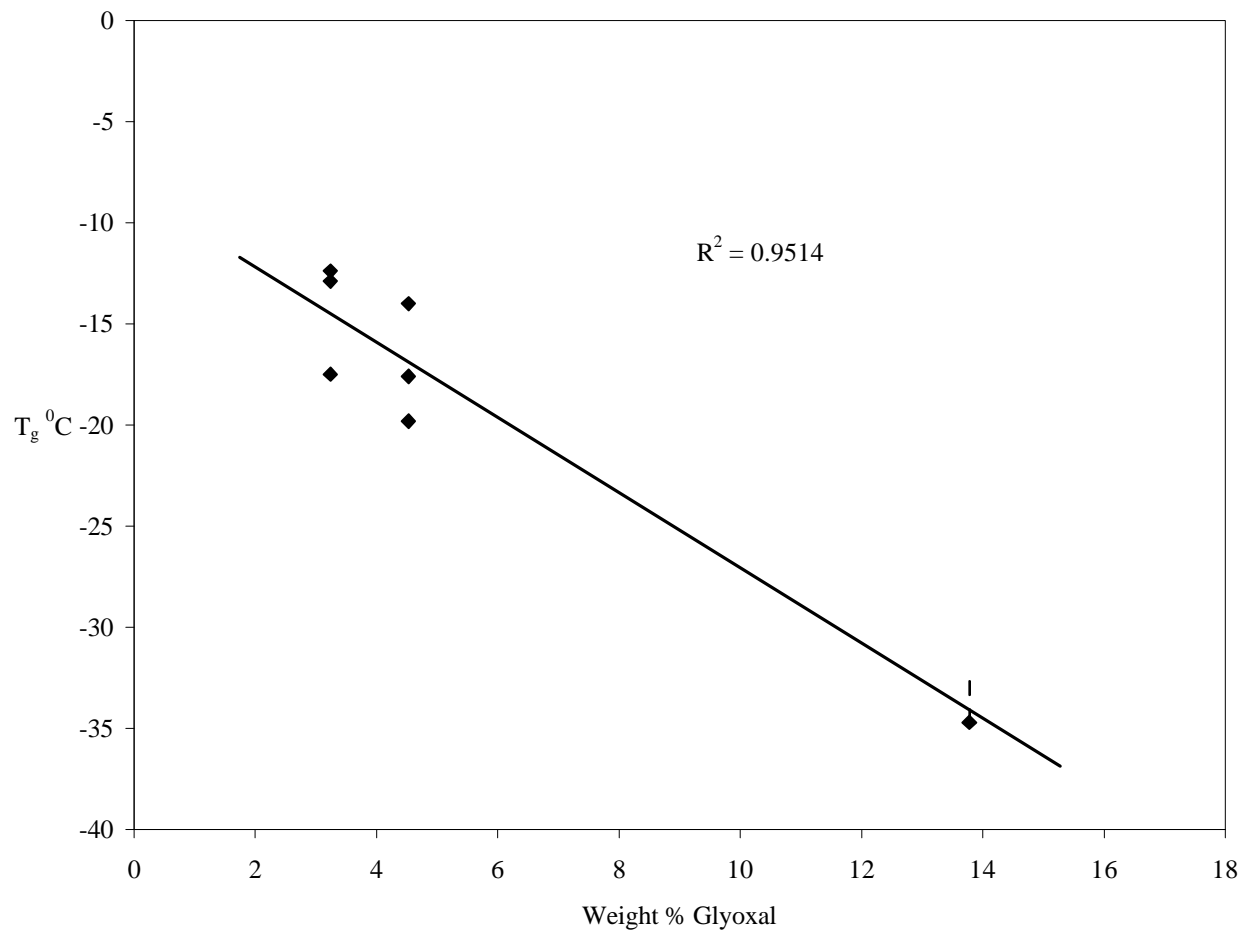


Figure 4.3.2 Dependence of glass transition temperature on glyoxal content for fresh frozen samples

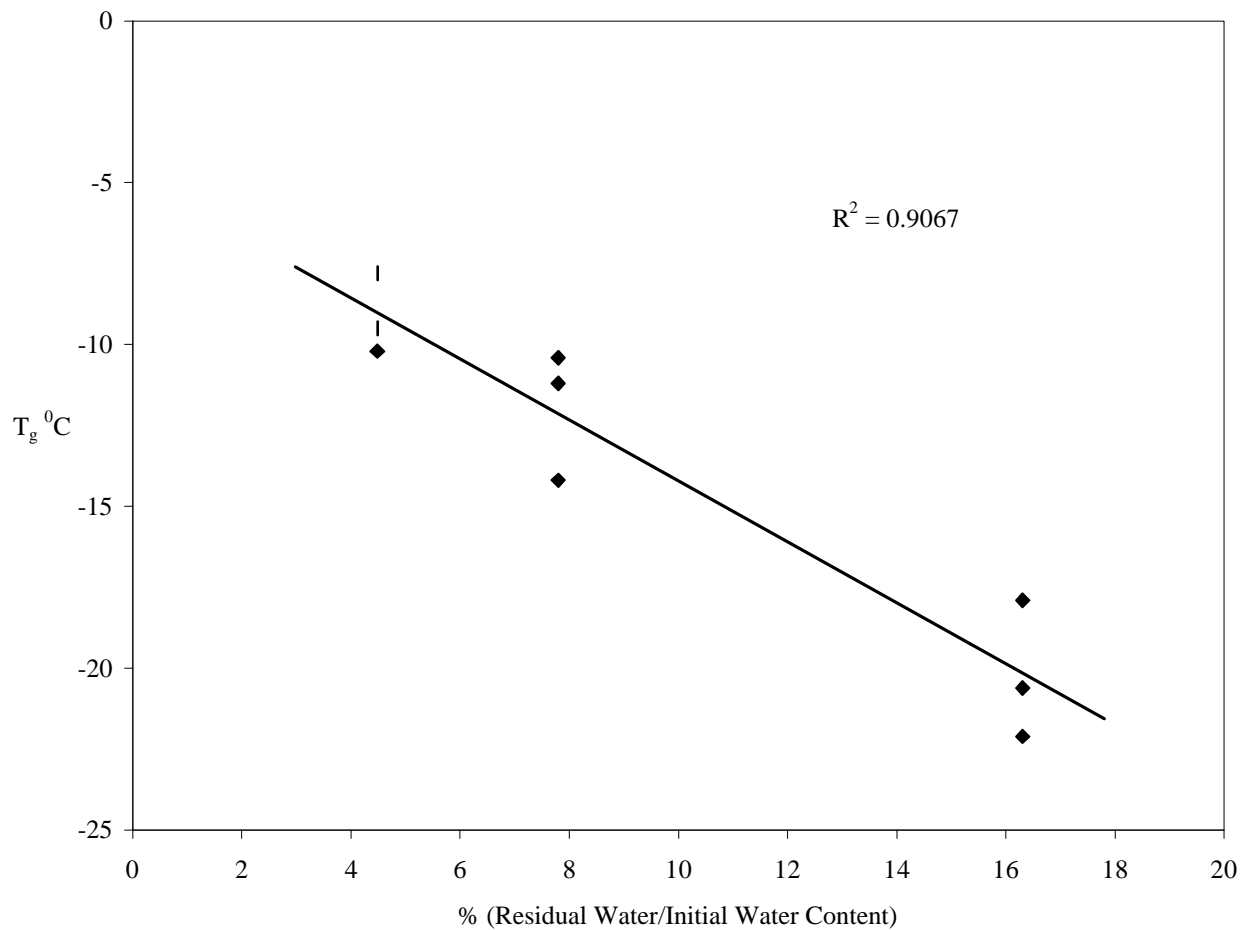


Figure 4.3.3 Graph of glass transition temperature of dried adhesives as a function of residual water content

4.3.2 DIFFERENTIAL SCANNING CALORIMETRY

Differential Scanning Calorimetry (DSC) could not identify the glass transition temperature because the expected T_g was hidden by the change in enthalpy for the melting of ice in the adhesives, Figure 4.3.4. However, this information could be used to determine the relative amount of unbound water liberated from the adhesives upon heating. The change in enthalpy for the melting of ice in the adhesives was compared among the formulations, Figure 4.3.5. The change in enthalpy of the ice melt decreased with increased glyoxal content in the adhesives. There was also a depression in the ice melt temperature with an increase in glyoxal content of the adhesives. The depression of the ice melt temperature was most evident for formulation G. This ice melting depression effect has also been noted in the literature, and is thought to be similar to the dissolution peak of ice in polymer solutions.³⁸ DSC was also conducted on samples of each formulation dried for 19-20 hours at 37⁰C. There were either no evident or very small peaks due to the melting of ice, suggesting that some unbound water evaporated during drying.

The critical concentration of water in the adhesive was increased by the addition of glyoxal, increasing the amount of water that was bound and decreasing the amount of unbound water that could be frozen. These results are in good agreement with the results of Ponomorova *et al.*³⁸ and Tenhu *et al.*⁴⁰ From our results, it can be inferred that less water was available to freeze because the balance was tightly bound within the bulk of the adhesives by glyoxal. The lack of an obtainable peak for dried samples supports evidence that unbound water was evaporated by drying at 37⁰C.

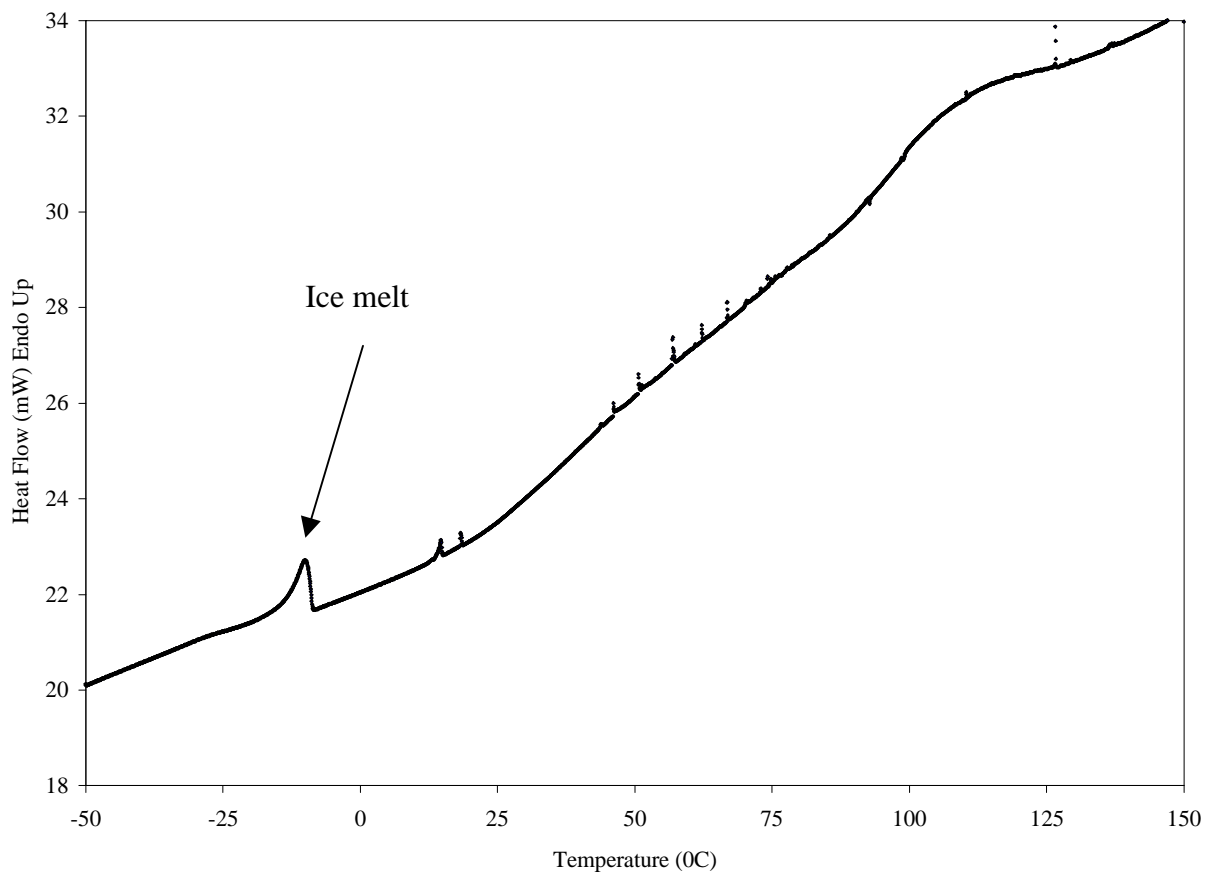


Figure 4.3.4 Typical DSC trace for adhesives

Table 4.3.2 Average measured change in enthalpy of ice melt at heating rates of 3⁰C/min and 10⁰C/min (J/g)

formulation C	formulation W	formulation G
16±2.3	20.3±3.0	10.6±1.1

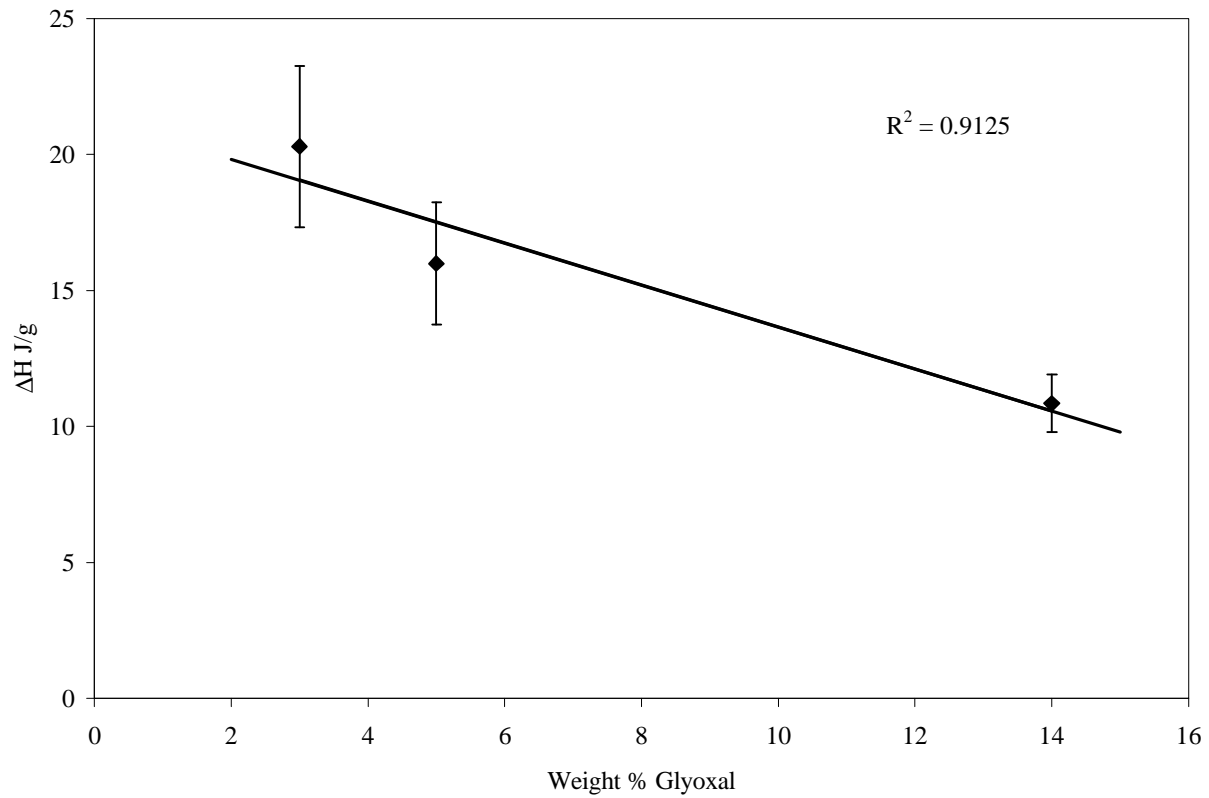


Figure 4.3.5 Change in enthalpy of the ice melt in adhesives as a function of glyoxal content

4.3.3 THERMOGRAVIMETRIC ANALYSIS

Thermogravimetric Analysis was conducted on samples that were freshly frozen and those that were dried for 19-20 hours at 37⁰C. The first derivative of the weight loss as a function of temperature was also analyzed using Microcal Origin 5.0. The weight loss as a function of temperature and the first derivative of the weight loss for fresh frozen samples are shown in Figure 4.3.6 and Figure 4.3.7. There are two distinct maxima of the first derivative around 50⁰C and 120⁰C for formulations C and G while for formulation W there was only one maximum around 50⁰C. A third maximum was observed above 300⁰C, but is associated with the weight loss due to decomposition of the adhesives. The weight loss as a function of temperature and first derivative of the weight loss for dried samples are shown in Figures 4.3.8 and 4.3.9. For dried samples, there was only one distinct maximum around 120⁰C. The maximum in weight loss of formulation G at 120⁰C is more pronounced than for the other formulations. The weight loss of the formulations in the temperature ranges of 25⁰C-100⁰C and 100⁰C-225⁰C corresponding to the evaporation of bound and unbound water is shown in Table 4.3.5. The weight loss in the temperature range of 100⁰C-225⁰C for formulation G (both dried and fresh frozen) was greater than the weight loss of formulations W and C. This corresponds to a higher content of bound water that exists in formulation G, which is the most cross-linked formulation. The results suggested that bound water is evaporated from the adhesives at temperatures above 100⁰C while unbound water is evaporated at temperatures below 100⁰C.

Thermogravimetric analysis revealed that higher temperature weight loss is due to bound water. The weight loss of formulation G with increased glyoxal content had in general a greater weight loss in the temperature range of 100⁰C -225⁰C when tested fresh and dried. The results are somewhat different than those obtained by Apostolov *et al.*³⁷ who concluded that bound water was lost in the temperature range of 25⁰C to 300⁰C, and Farikov *et al.*⁴¹ who concluded that bound water was evaporated in the range of 150-170⁰C. An accurate temperature range for the evaporation of both bound and unbound water may not be obtainable since there was an overlap in the peaks of the first derivative curve for fresh frozen samples. Another consideration is that weight loss due to evaporation of water from the adhesives started instantaneously after removal from the freezer, as noted by the small difference in weight measured by the instrument prior to testing and the measurements made at the beginning of the tests. Perhaps if

thermogravimetric analysis could begin at sub-ambient temperatures, a more accurate analysis could be conducted for these adhesives.

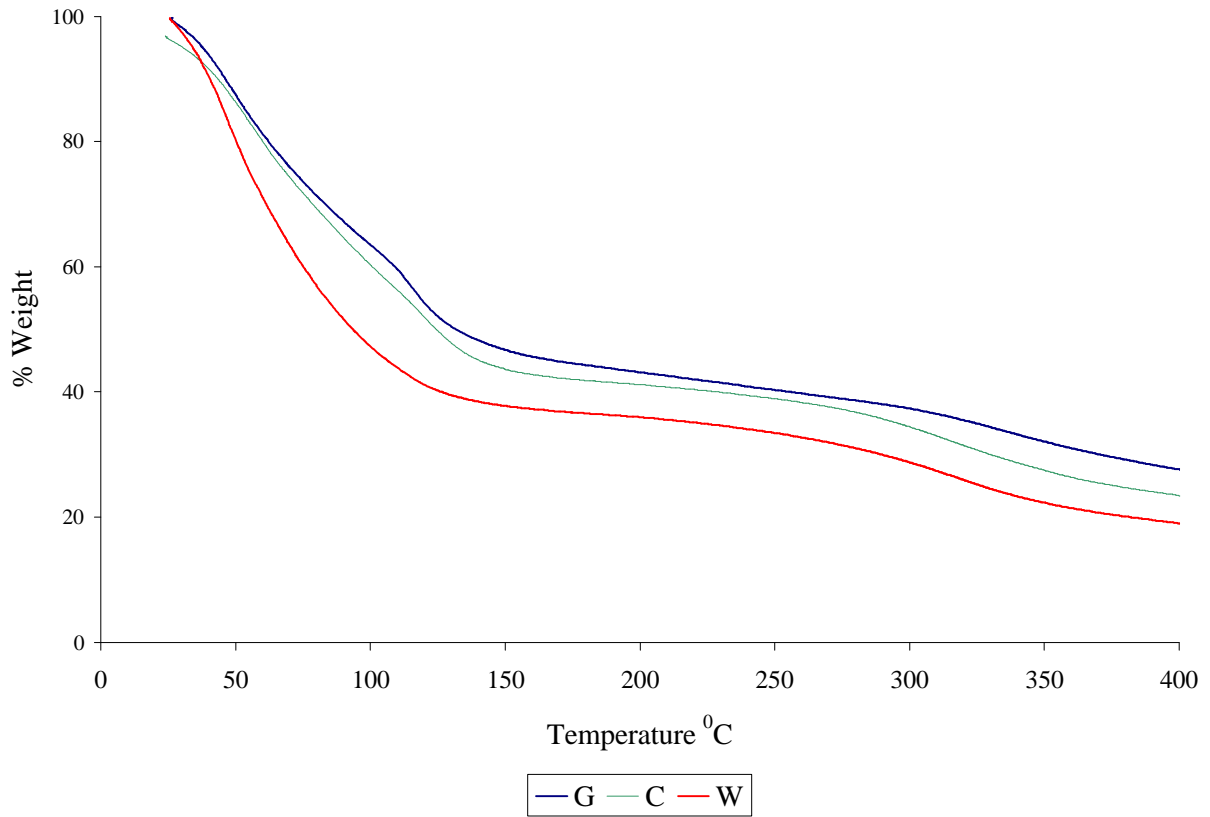


Figure 4.3.6 Representative weight loss thermogram for fresh frozen samples

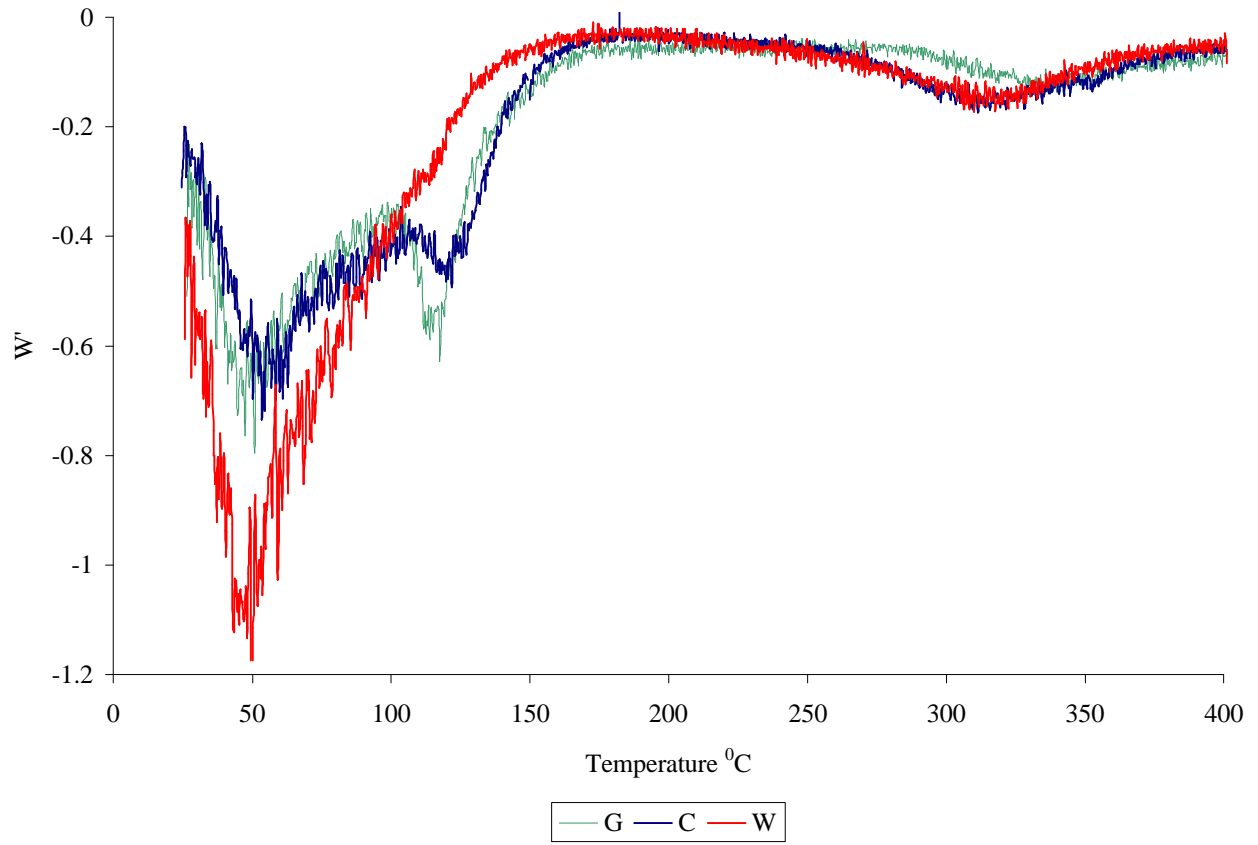


Figure 4.3.7 First derivative of weight loss of fresh frozen samples

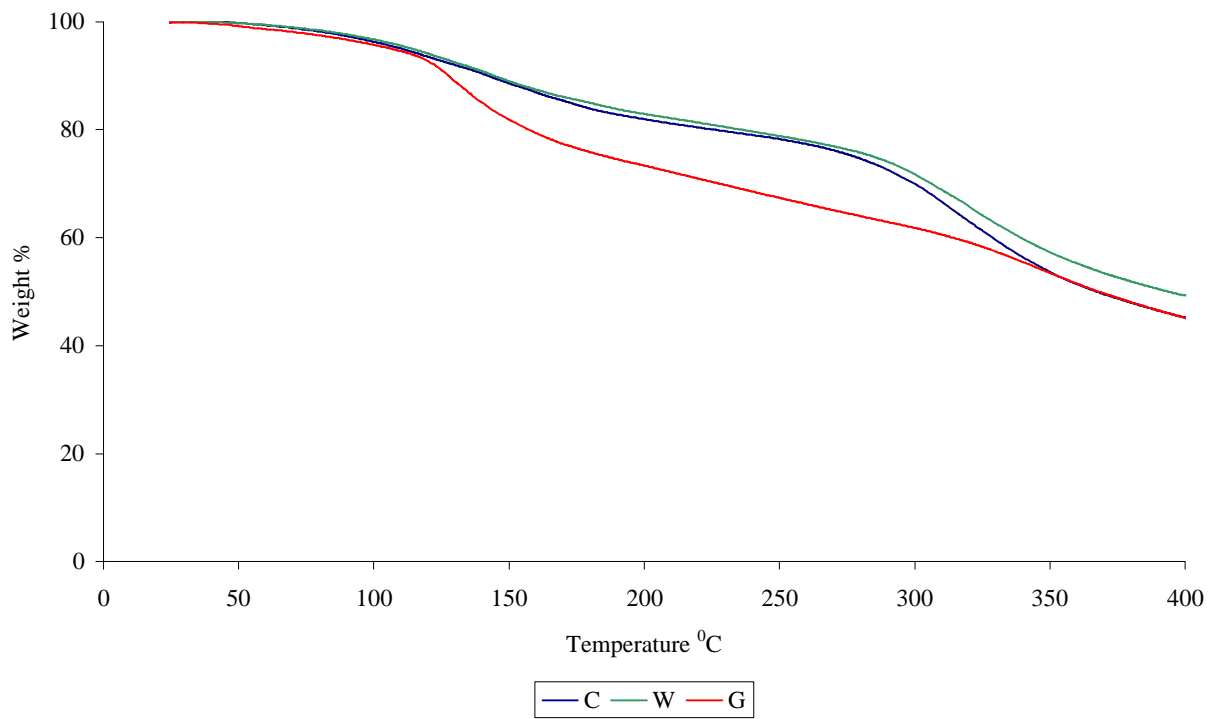


Figure 4.3.8. Representative weight loss thermogram for dried samples

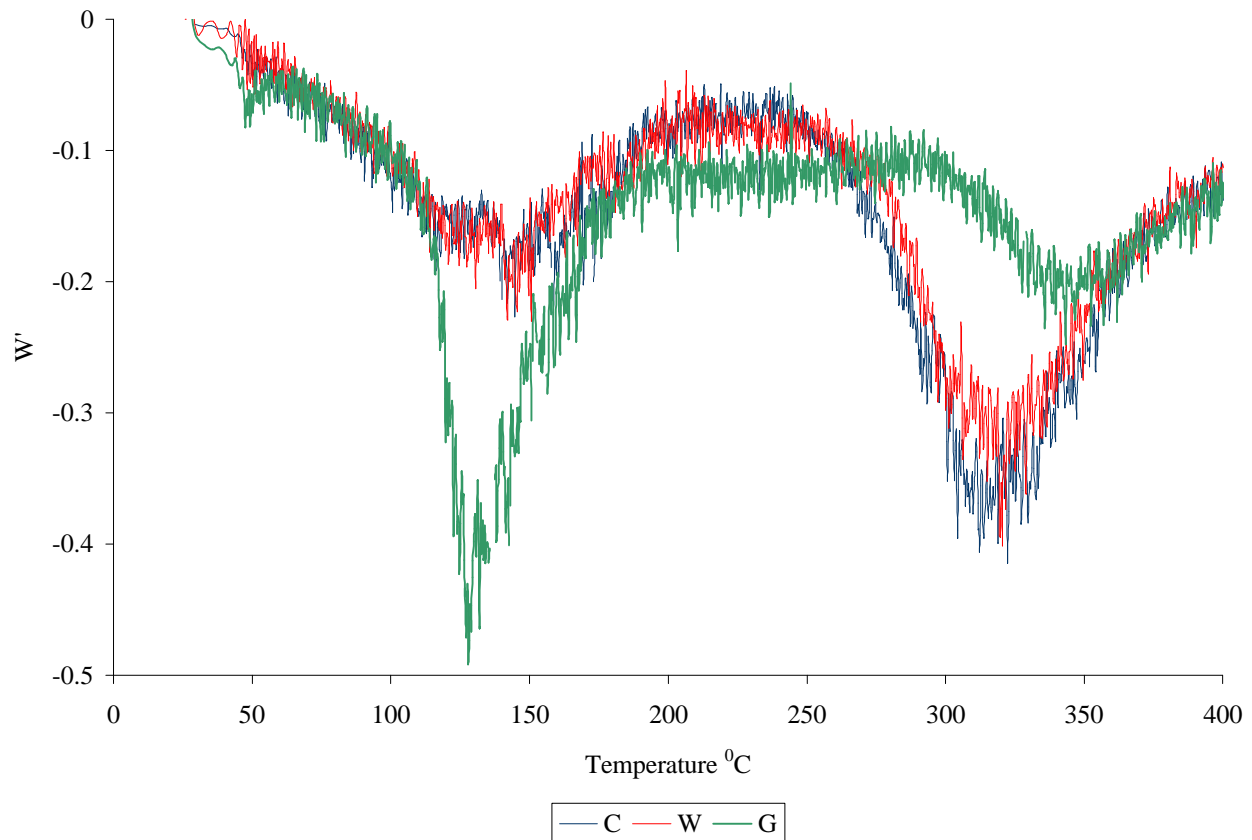


Figure 4.3.9 First derivative of weight loss of dried samples

Table 4.3.3 Weight loss as a function of temperature for dried and fresh frozen samples

Temperature Range	Change in Weight					
	C	C dried	W	W dried	G	G dried
25-100 ⁰ C	39%	4%	54%	3%	37%	4%
100-225 ⁰ C	19%	16%	16%	16%	21%	26%

4.4 OPTICAL MICROSCOPY OF ADHESIVES

Results from drying and thermal analysis suggest the existence of bound water in the adhesives. Using optical microscopy and samples that exhibited phase segregation due to improper mixing, the bound and unbound water phases could be identified as shown in Figure 4.4.1.

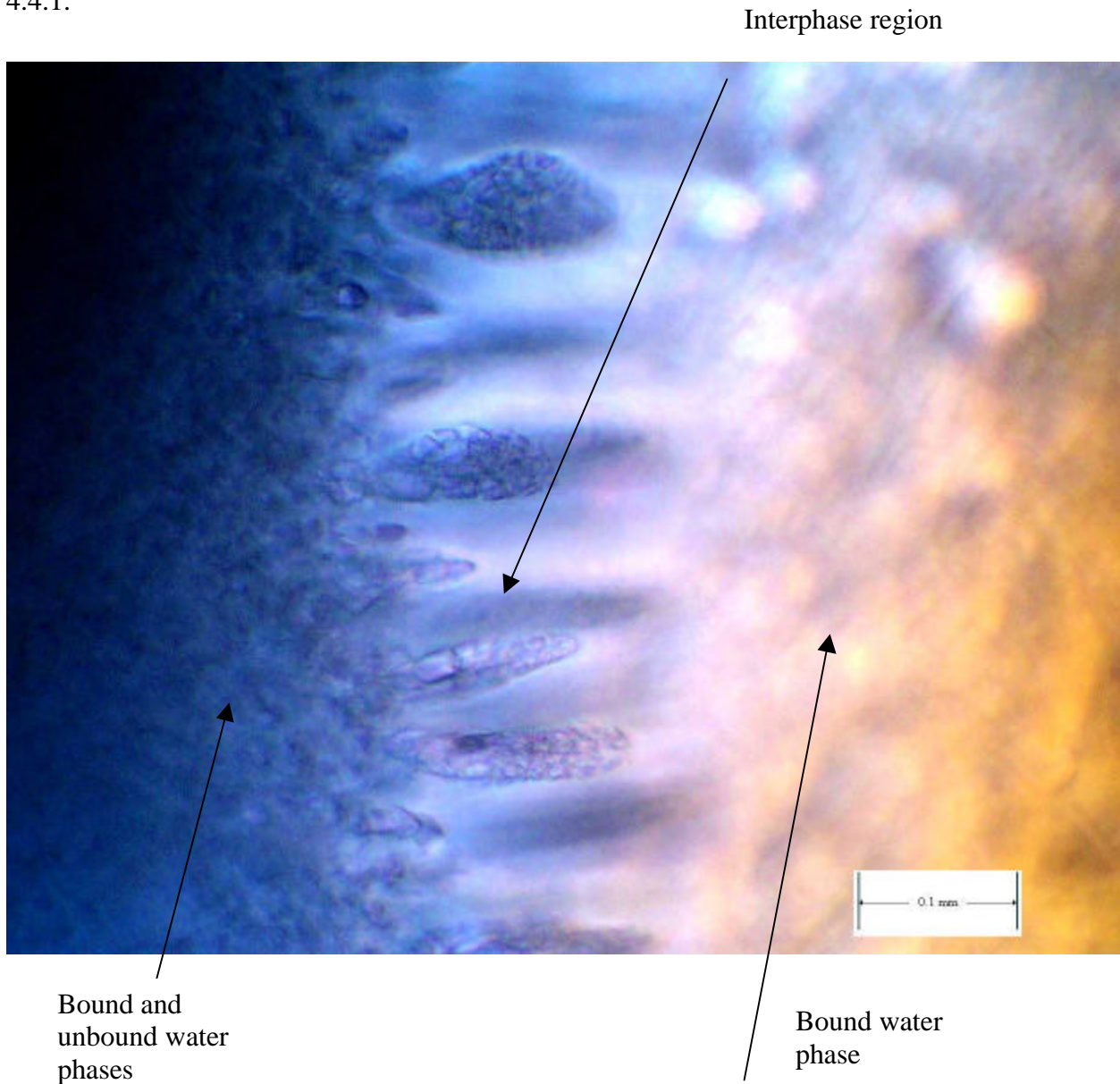


Figure 4.4.1 Optical micrograph of bulk adhesive showing bound and unbound water phases

4.5 MECHANICAL TESTING OF ADHESIVES

4.5.1 TENSILE TESTING

The engineering stress of each sample was calculated as the force per unit initial cross sectional area, $\sigma = \frac{F}{A_c}$. The engineering strength of the material was determined at the highest force recorded. The elastic modulus was calculated as the slope of the linear portion of the stress strain curve as ϵ approaches zero, using Microcal Origin software. The strain at break was chosen at the corresponding strain to the highest force recorded prior to break. Typical stress strain curves for fresh frozen samples of each formulation are shown in Figure 4.5.1. Tensile testing was also conducted on samples that had been dried for 19-20 hours at 37°C, and typical stress strain curves are shown in Figure 4.5.2. The strength, elastic modulus, and strain at break of dried and fresh frozen adhesive formulations are summarized in Table 4.5.1. For fresh frozen samples, formulation C had the highest average strength and elastic modulus, but lower average strain at break compared to formulations W and G. Formulation G was weaker and more compliant than the control formulation, while formulation W only had a significantly lower modulus than the control formulation. There were no significant differences amongst formulations for the strain at break. A possible explanation for the higher modulus and strength of the control formulation compared to the other formulations is the incidence of hydrogen bonding between protein molecules. Since formulation C had a higher weight content of gelatin than formulations G and W, the existence of hydrogen bonding between the protein chains is increased which would support the results of higher strength and modulus. The higher average modulus of formulation G compared to formulation W may be due to increased covalent cross-linking. A plot of the strength and modulus as a function of gelatin content is given in Figure 4.5.3.

When the adhesives were dried, they became brittle in comparison to the fresh frozen adhesives as noted by the increase in strength and modulus, and the decrease in the strain at break. The brittle behavior resulting from drying was a result of the water lost from the adhesives. Since bound water is not evaporated at 37°C, the adhesives with more bound water

will become less brittle after drying in comparison to adhesives with less bound water. The strength and modulus of the dried adhesives as a function of residual or bound water content are shown in Figure 4.5.4. The strain at break increased linearly with increasing residual water content in the adhesives and is shown in Figure 4.5.5. Following drying, formulation W had the highest average strength and elastic modulus, and lowest strain at break compared to formulations C and G. Formulation W had significantly greater strength and modulus than formulation C when dried because it contained the least bound water and most unbound water. Following drying, formulation G had significantly greater strength compared to formulation C most likely due to increased number of chemical cross-links, and significantly greater strain at break, due to the inclusion of the most bound water for the adhesive formulations. In conclusion, formulation W became the most brittle after aging compared to formulations C and G.

The mechanical properties of skin are quite variable and are given in Table 4.5.2. The values of the elastic modulus are between 6.4 to 44 MPa, values of the strength are between 4.00 to 14.00 MPa, and values of the strain at break are between 0.80 and 1.00.⁹ The adhesive is weaker but more compliant than skin when fresh, but following drying, the strength and modulus approach the values for skin, but the elongation at break of skin is much smaller than the adhesive.

Table 4.5.1 Average measured strength, elastic modulus, and strain at break by formulation

Fresh Frozen	Strength (kPa)	Modulus (kPa)	Strain at Break
C	63±8.2	14±3.3	7.2±0.50
W	52±12	8.0±0.69*	8.2±1.9
G	49±4.9*	9.2±0.34*	8.2±1.2
Dried	Strength (kPa)	Modulus (kPa)	Strain at Break
C	950±140	27000±5800	0.071±0.016
W	2000±270*	61000±16000*	0.057±0.026
G	1200±210*	21000±6300	0.14±0.053*

* Statistically significant against formulation C

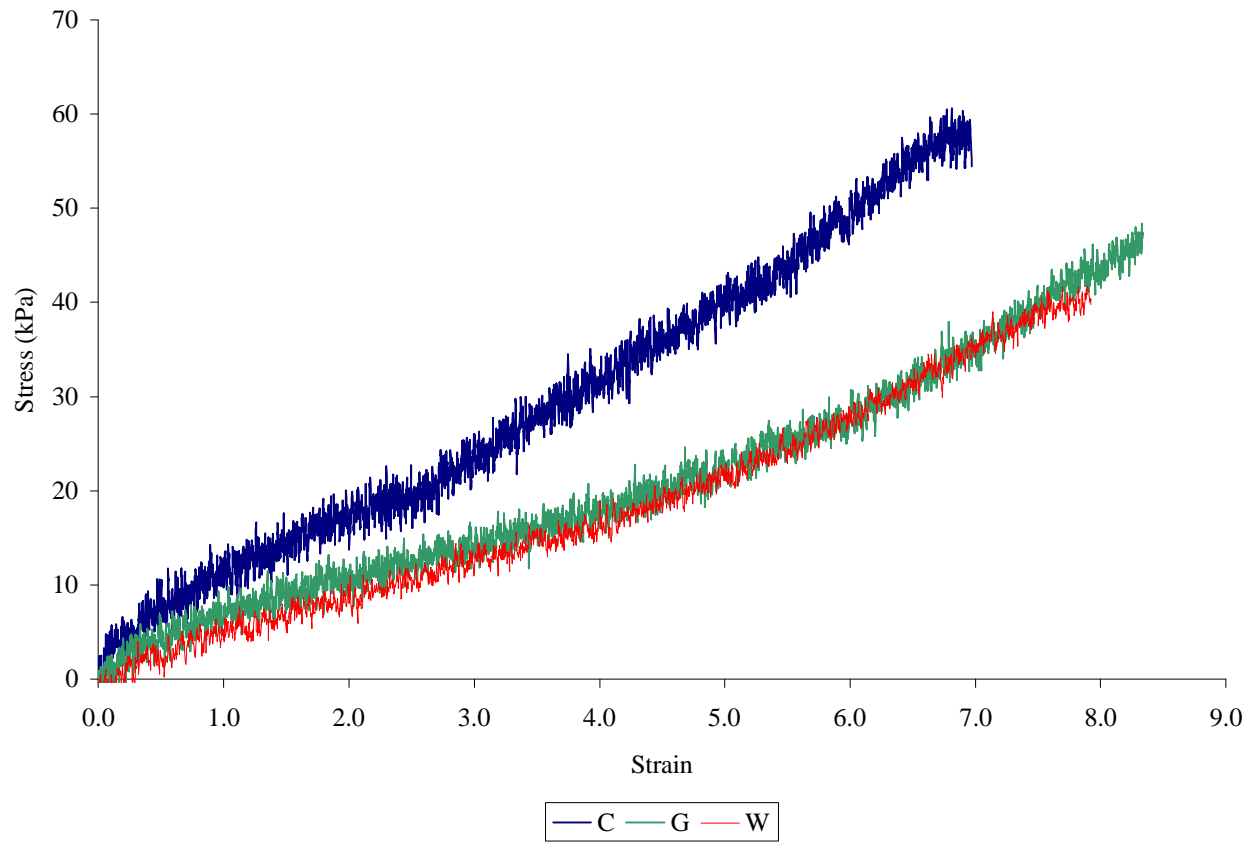


Figure 4.5.1 Typical stress-strain curves for fresh frozen samples

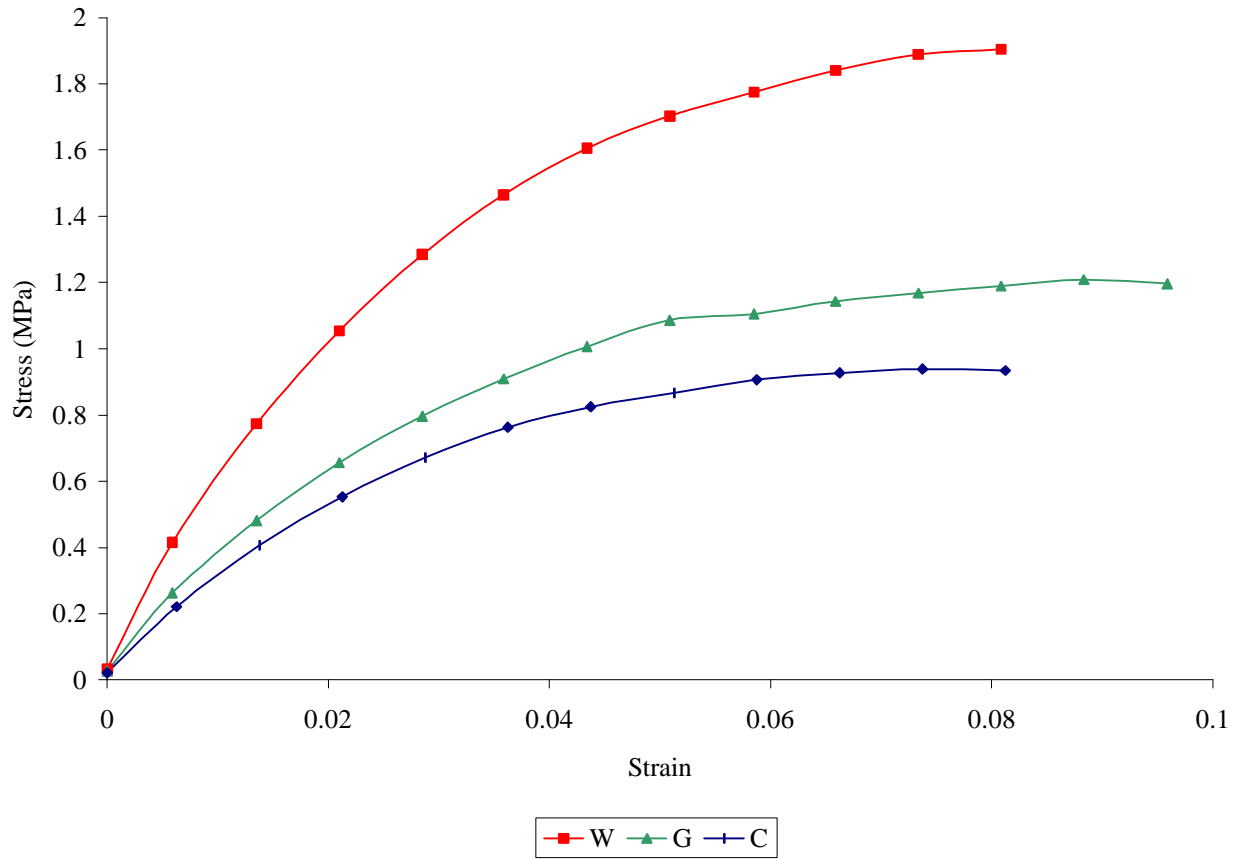


Figure 4.5.2 Typical stress-strain curves for dried samples

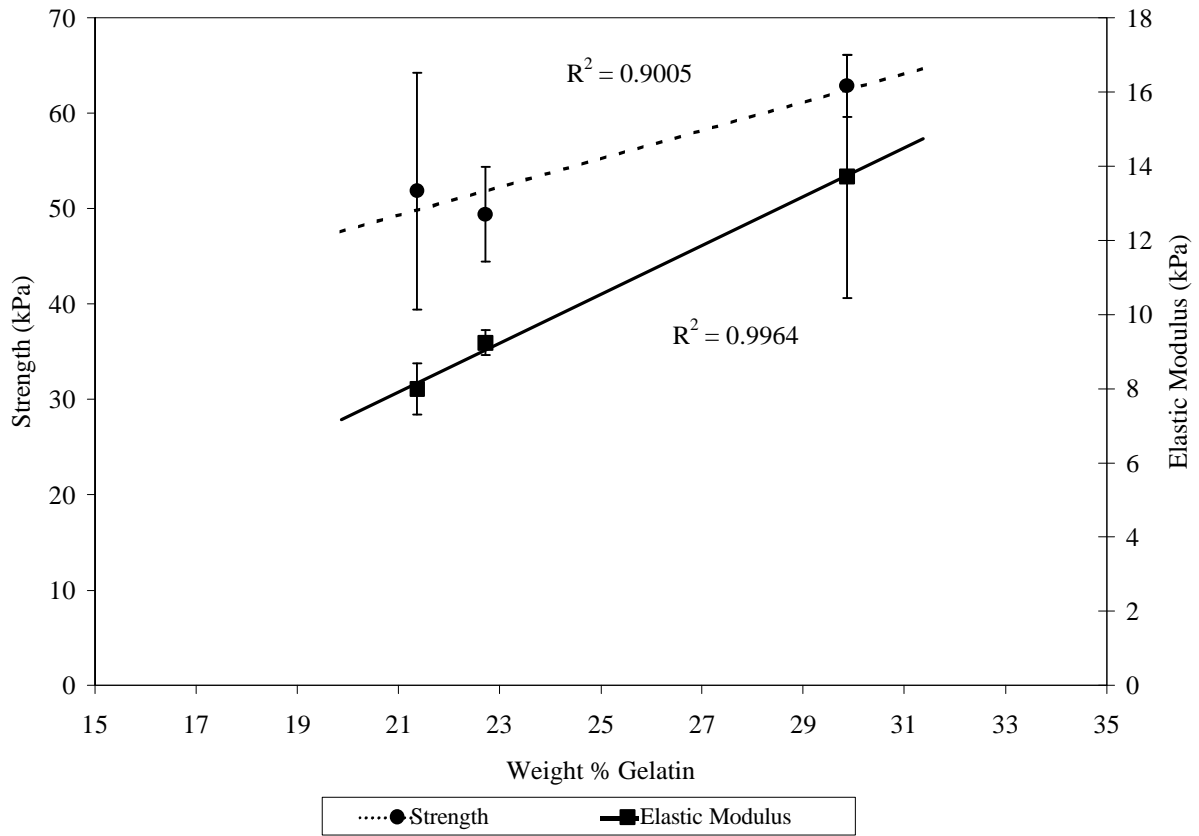


Figure 4.5.3 Graph of strength and elastic modulus dependence on gelatin weight % for fresh frozen adhesives

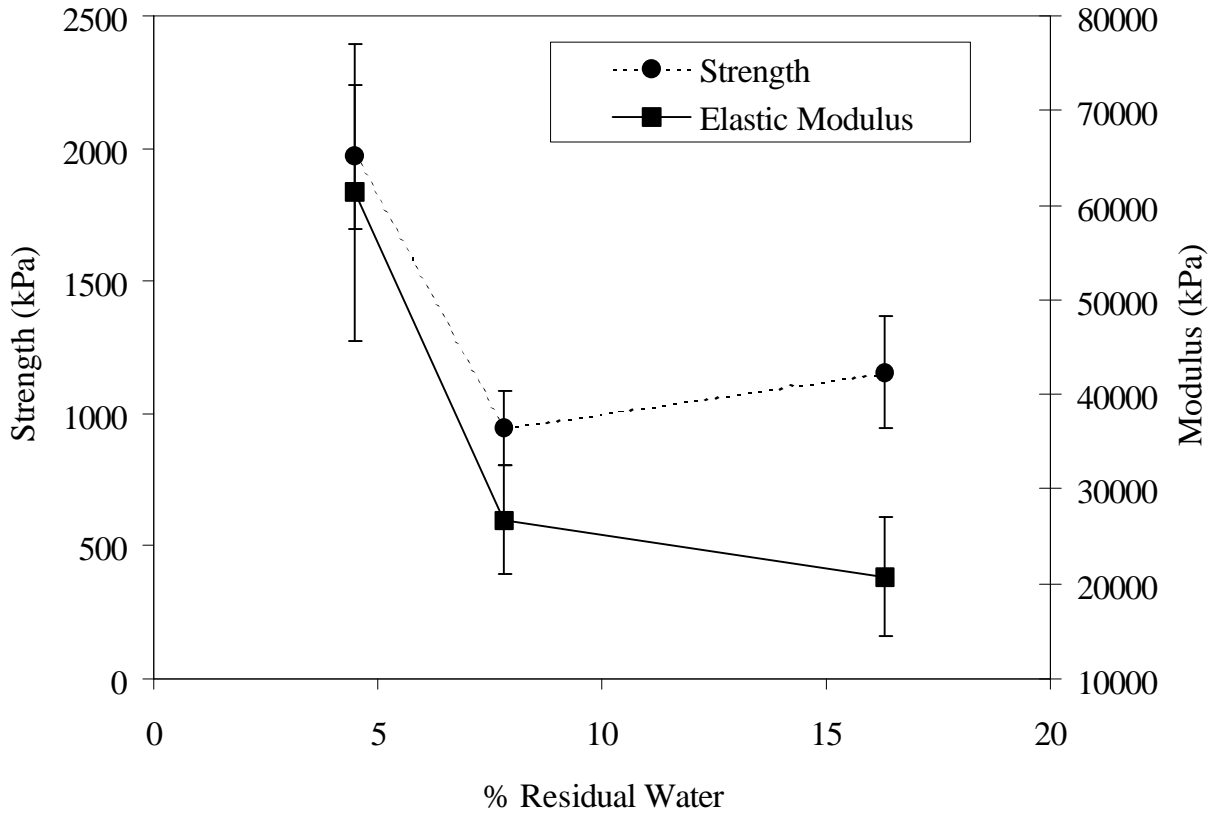


Figure 4.5.4 Graph of strength and modulus of dried adhesives as a function of residual water content

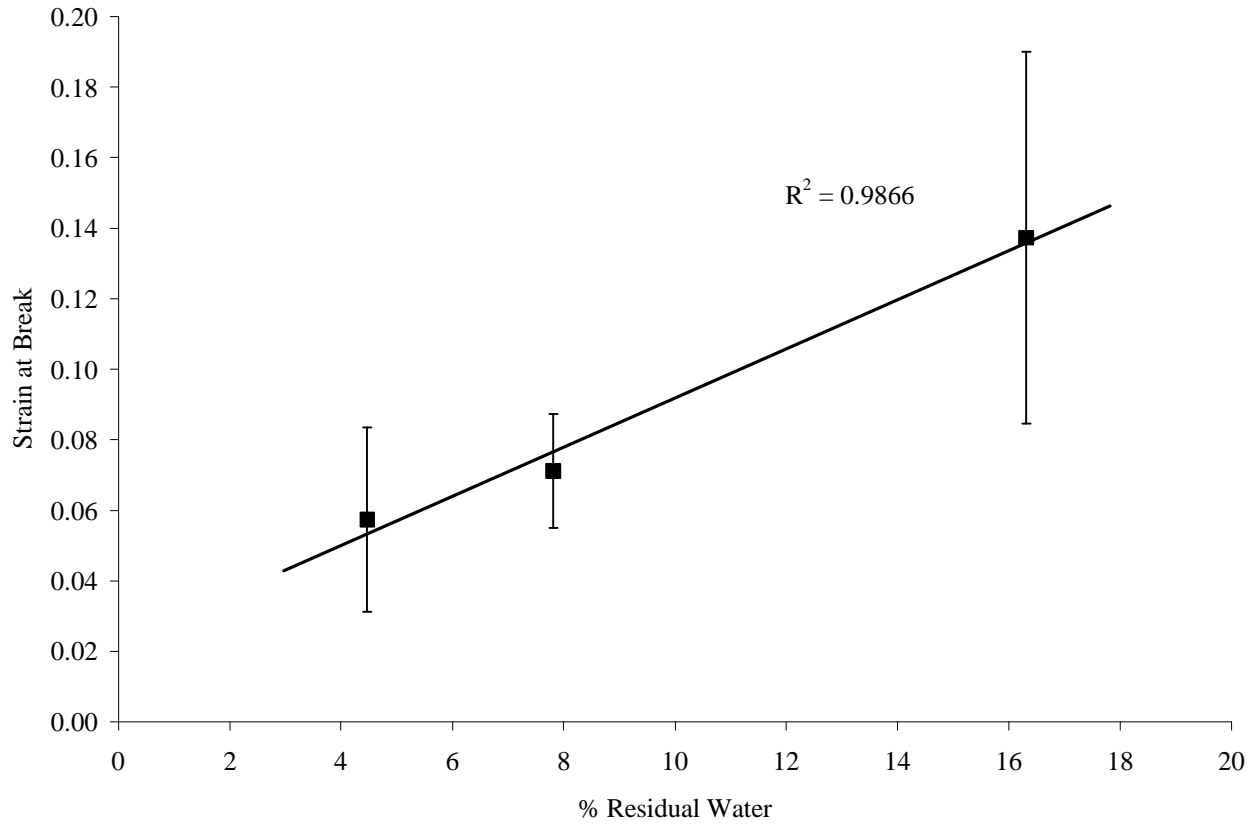


Figure 4.5.5 Graph of strain at break as a function of residual water content of dried adhesives

Table 4.5.2 Table of mechanical properties of skin⁷

Tissue	Failure strain ϵ_f	Failure strength σ_f	Modulus
Abdominal skin (human)	1.00	14.00 MPa*	22.4 MPa*
	0.80	4.00 MPa	-
Back skin (rat)	-	-	1-2 kPa
	0.90	5.00 MPa*	6.4 MPa*
Back skin (rat) (12 months)	1.00	12.50 MPa	44 MPa

• calculated using true stress

4.5.2 STRESS RELAXATION

The stress relaxation data was fit to an empirical two element exponential decay model corresponding to $\frac{\mathbf{s}}{\mathbf{s}_o} = \mathbf{s}_\infty + A_1 \exp^{-t/t_1} + A_2 \exp^{-t/t_2}$ given as equation 2.8.9 where A_1 represents a pre-exponential constant corresponding to the first relaxation time t_1 , and A_2 represents a pre-exponential constant corresponding to the second relaxation time t_2 . The data was fit using Microcal Origin 5.0 software with minimization in chi-squared. A graph of a typical relaxation curve of the adhesives is shown in Figure 4.5.6. The average relaxation fit parameters by formulation are given in Table 4.5.3. The average stress at infinite time, σ_∞ , for formulation G was lower than for formulations C and W. The average first relaxation time τ_1 for formulation C was greater than for formulations W or G. However, the average pre-exponential constant A_1 for the first relaxation time of formulation G was greater than for formulations C and W, indicating a greater dependence on the first relaxation time. The values for the second relaxation time and pre-exponential constant are comparable among the formulations. A plot of the relaxation behavior of all three formulations using average values for the fit parameters is shown in Figure 4.5.7. The relaxation time terms t_1 and t_2 correspond to the fraction of viscous and elastic terms ($\frac{h}{E}$) of the Maxwell model. The average first relaxation time t_1 for formulation C was significantly greater than formulations G and W, and likely was a result of intermolecular friction between the large protein chains, since this formulation had the highest gelatin content. Formulation G had the lowest average first relaxation time (t_1), and the largest pre-exponential constant A_1 compared to formulations C and W. This was likely a result of increased elasticity due to cross-linking and decreased intermolecular friction resulting from the bound water in the adhesive. The average values for the second relaxation time (t_2) and pre-exponential constant (A_2) were comparable. The non visco-elastic term or relaxed stress (\mathbf{s}_v) for formulation G was significantly lower than both formulations C and W likely resulting from the plasticizing effect of bound water within the adhesive.

Table 4.5.3 Average relaxation fit parameters by formulation

	C	W	G
σ_{∞}	0.35±0.06	0.35±0.05	0.22±0.03*
A_1	0.21±0.08	0.20±0.03	0.28±0.06
τ_1 (seconds)	16±8.6	9.6±2.2*	8.5±3.1*
A_2	0.51±0.14	0.41±0.09	0.46±0.06
τ_2 (seconds)	360±100	370±45	330±60

* Statistically significant against formulation C

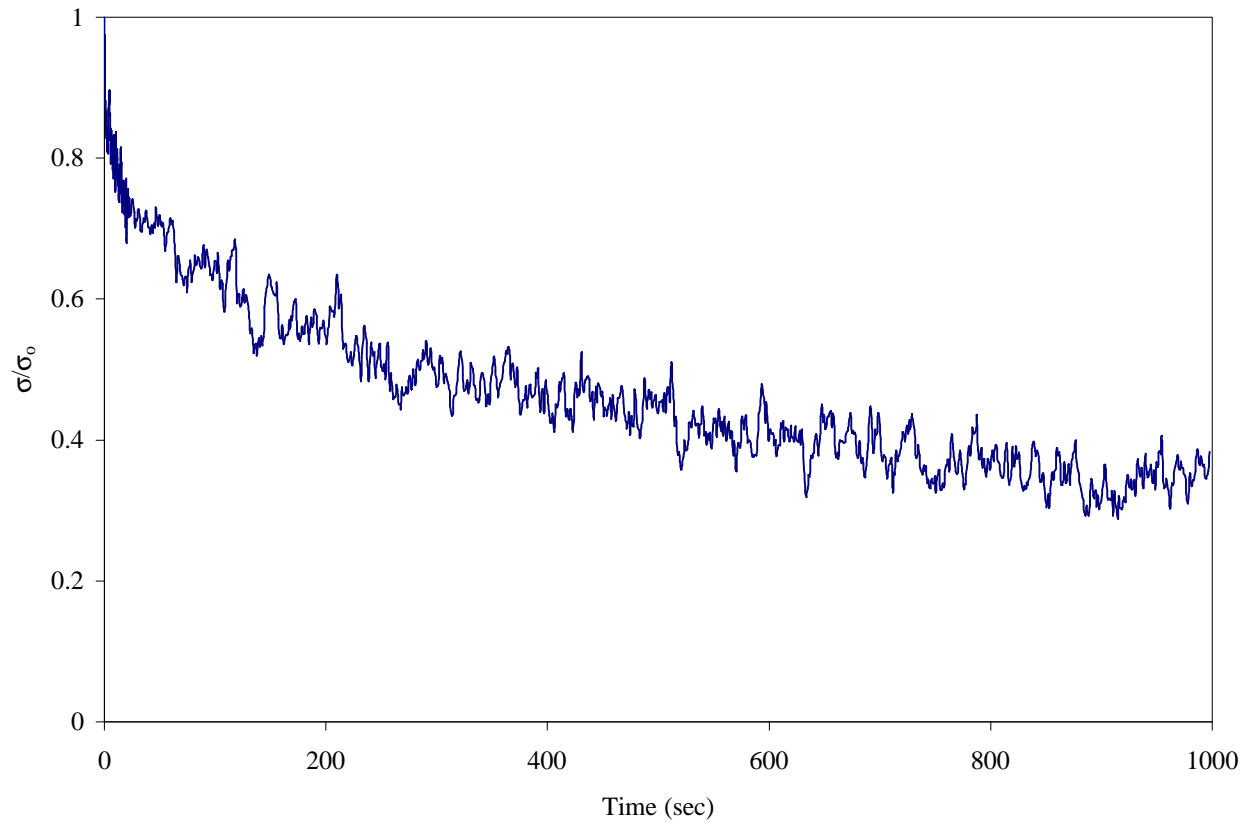


Figure 4.5.6 Typical stress relaxation curve

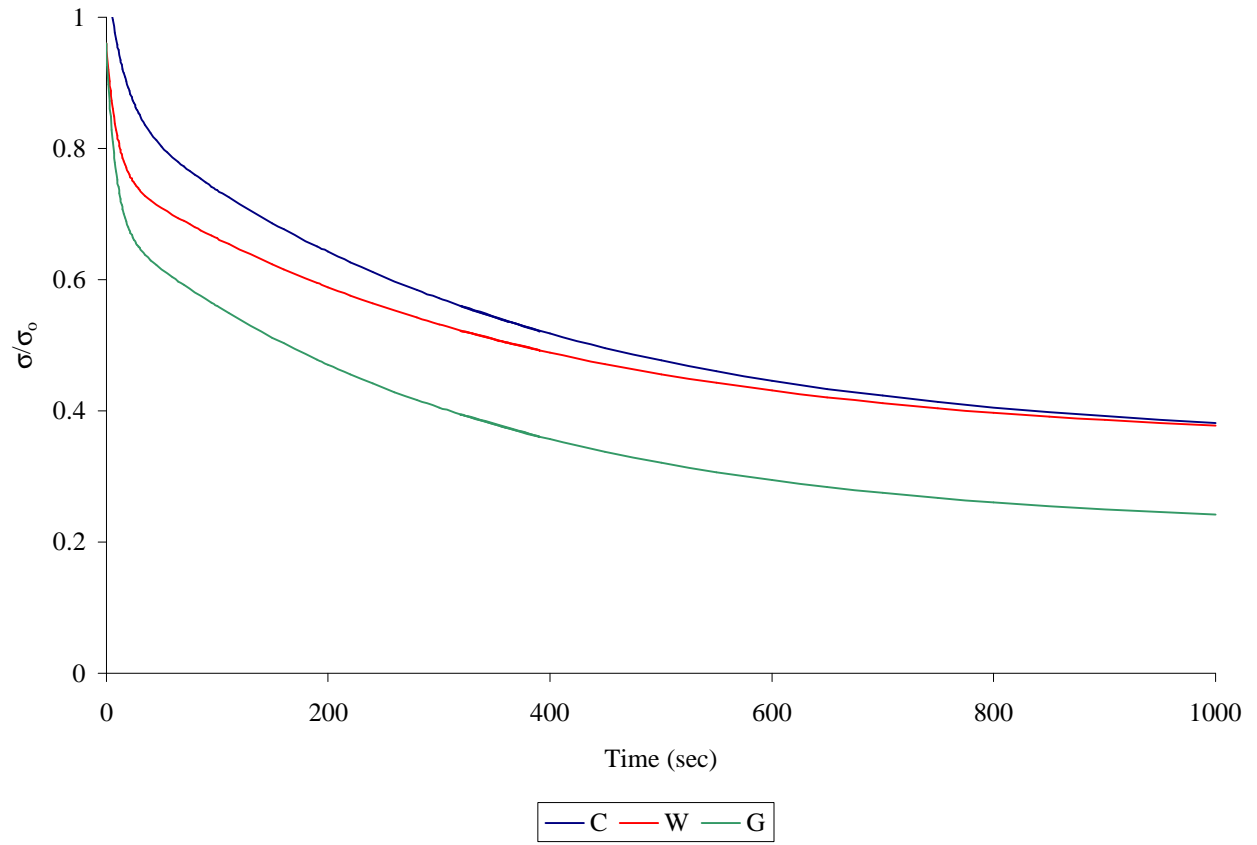


Figure 4.5.7 Graph of relaxation behavior of the three formulations using average fit parameters

4.6 ADHESIVE TESTING

4.6.1 LAP SHEAR TESTING OF ADHESIVE BONDED GLASS SUBSTRATES

Lap shear adhesive testing was conducted on glass slides bonded with adhesive. The average shear stress was calculated by dividing the force by the bond area. Typical stress versus distance curves for fresh samples bonded to glass are shown in Figure 4.6.1. Lap shear samples that were dried for 19-20 hours at 37⁰C were also tested. Typical stress versus distance curves for dried lap shear samples of all formulations are shown in Figure 4.6.2. The average measured shear strength for all samples that were tested are shown in Table 4.6.1. Formulation C had the highest average shear strength for both the dried and fresh lap shear tests.

The adhesive strength of the fresh and dried lap shear bonds increased with increased gelatin content, similar to the trend observed for the strength of the fresh frozen adhesives, Figure 4.6.3. Formulation C had both the highest strength and highest adhesive strength. The increase in adhesive strength with gelatin content is also likely due to hydrogen bonding since hydrogen bonding between gelatin and substrate has been implicated as an adhesion mechanism of hybrid tissue adhesives.^{4,5} Another possible reason that the strength and adhesive strength of formulation C are comparably the greatest may be because the strength of an adhesive bond is largely dependent on the cohesive strength of the adhesive.⁴⁷ For dried lap bonds, the visible drying of the adhesives on the outer edges of the bond area was a result of diffusion of water from the outer edges due to contact of these surfaces with air. The water in the interior portions of the adhesive bond was unable to diffuse through the outer portions of the bond. Volkersen's equation (2.9.12) for stress concentrations at edges of the bond length were found to be negligible for the fresh lap bonds since the modulus of the glass slide adherends (69 GPa) was much greater than the shear modulus of the adhesives (3-5 kPa). Stress concentrations at the edges of the bond length for dried lap bonds probably exist due to the non-uniform drying and shrinkage of the adhesives at the outer edges, but could not accurately be assessed using Volkersen's equation. In addition, the stress concentrations could not be assessed using Volkersen's equation because the assumption that the shear modulus of the adhesive being equal to one third the elastic modulus would be incorrect since the dried adhesive no longer behaves like an elastomer.

Table 4.6.1 Table of average shear strength values for adhesive bonded glass substrates

	Shear Strength (kPa)		
	Formulation C	Formulation W	Formulation G
Fresh	23±15	15±5.5	16±5.5
Dried	110±12	80±12*	75±24*

* Statistically significant against formulation C

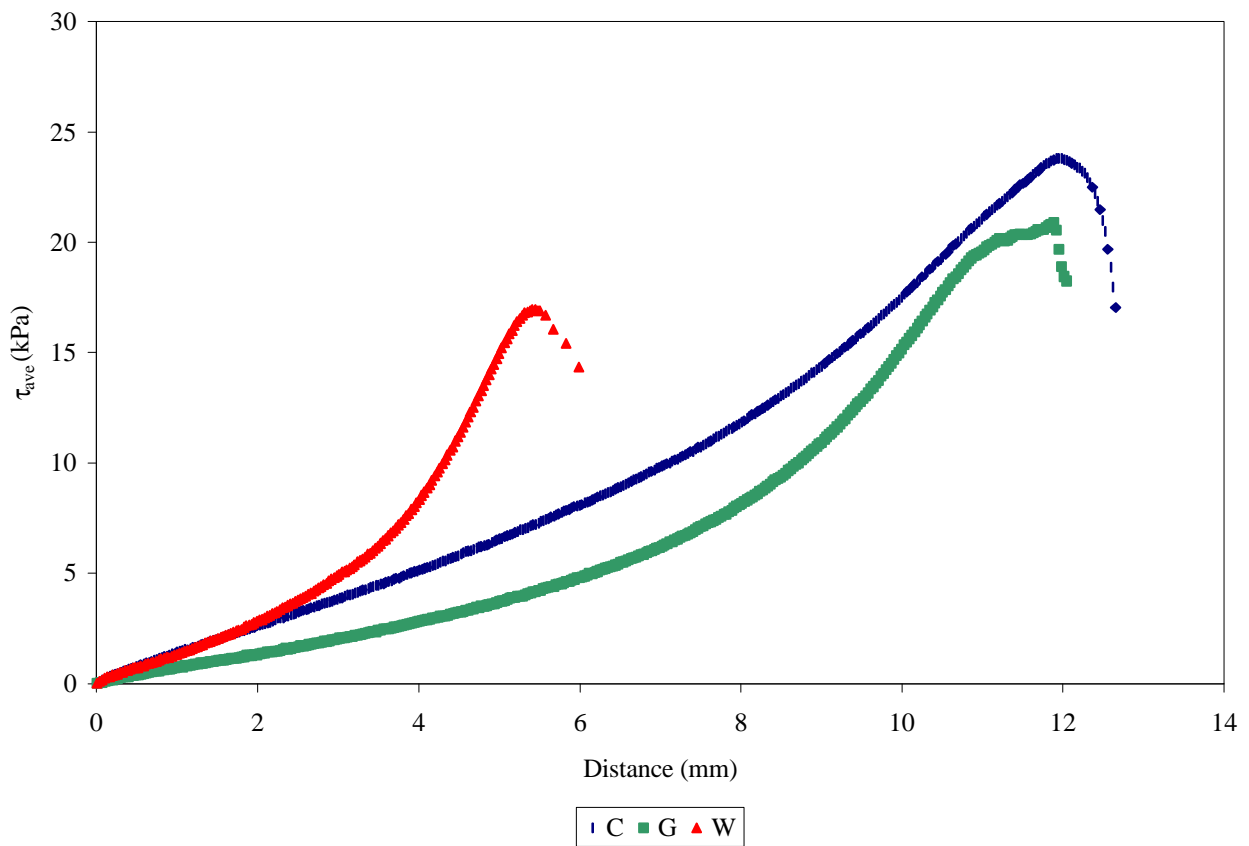


Figure 4.6.1 Typical average shear stress vs. distance curves for fresh lap shear samples

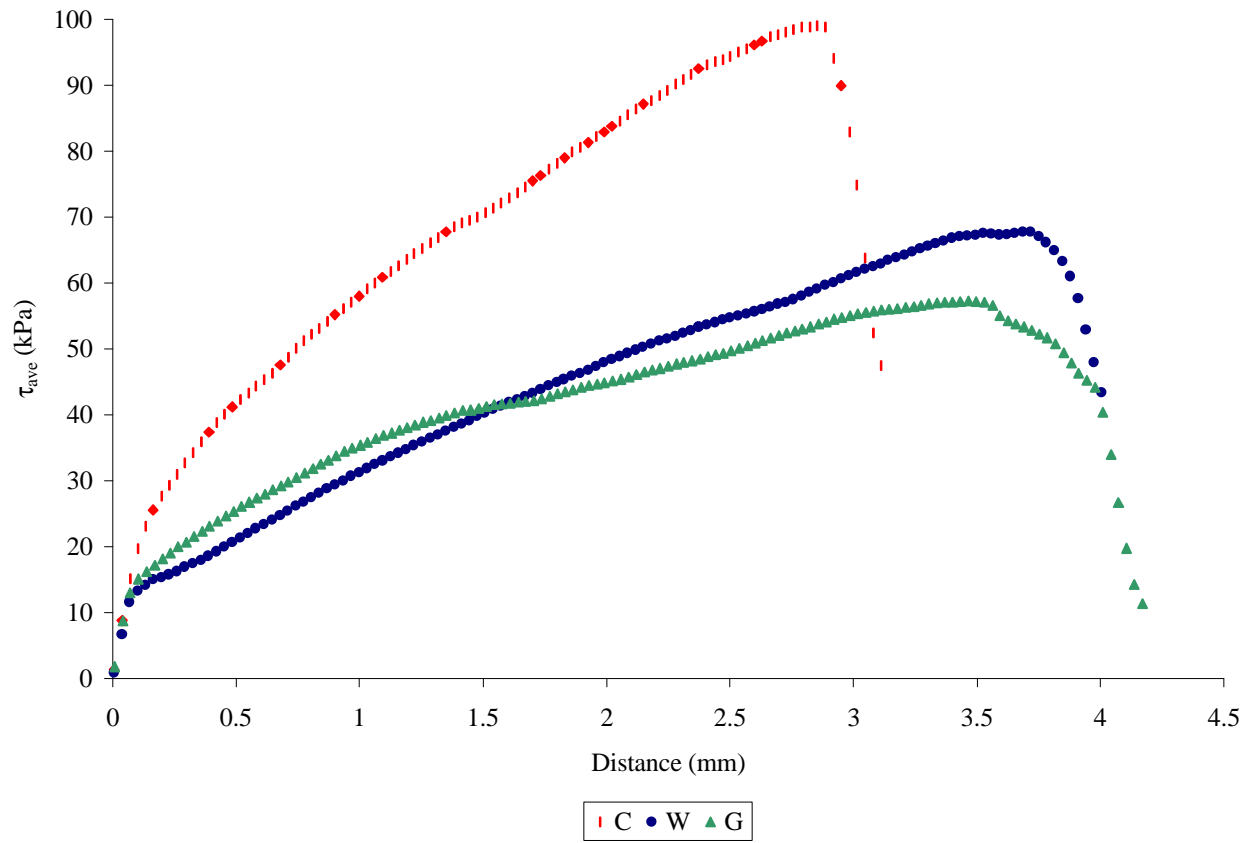


Figure 4.6.2 Typical average shear stress vs. distance curves for dried lap shear samples

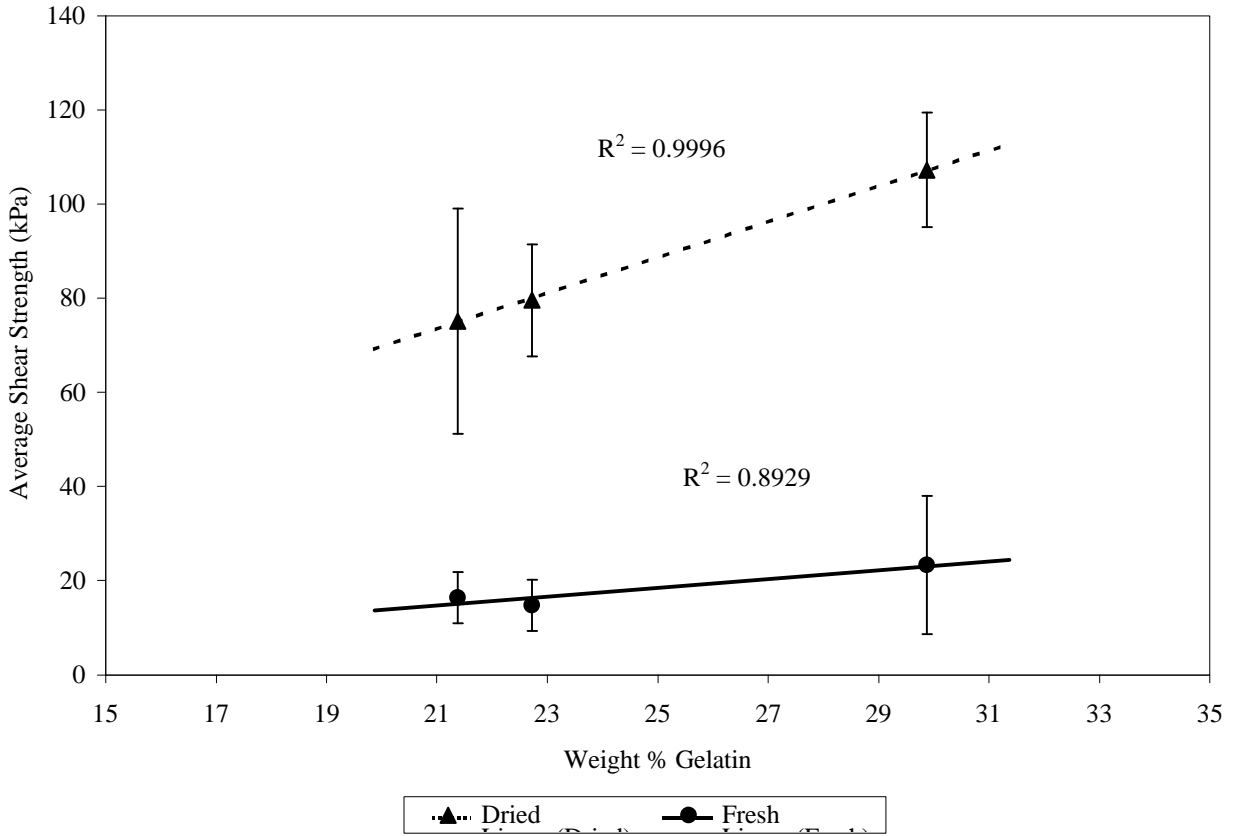


Figure 4.6.3 Graph of the average shear strength of lap shear bonds as a function of gelatin content

4.6.2 FAILURE OF ADHESIVE BONDS

The failure mode of the adhesive bonds was determined using optical microscopy. The lap bonds showed evidence of cohesive failure since there was adhesive found on the surface of the glass slides, Figure 4.6.4. Cohesive failure is a common failure mode denoted for other adhesives in the literature, (Refer to Figure 2.9.4).

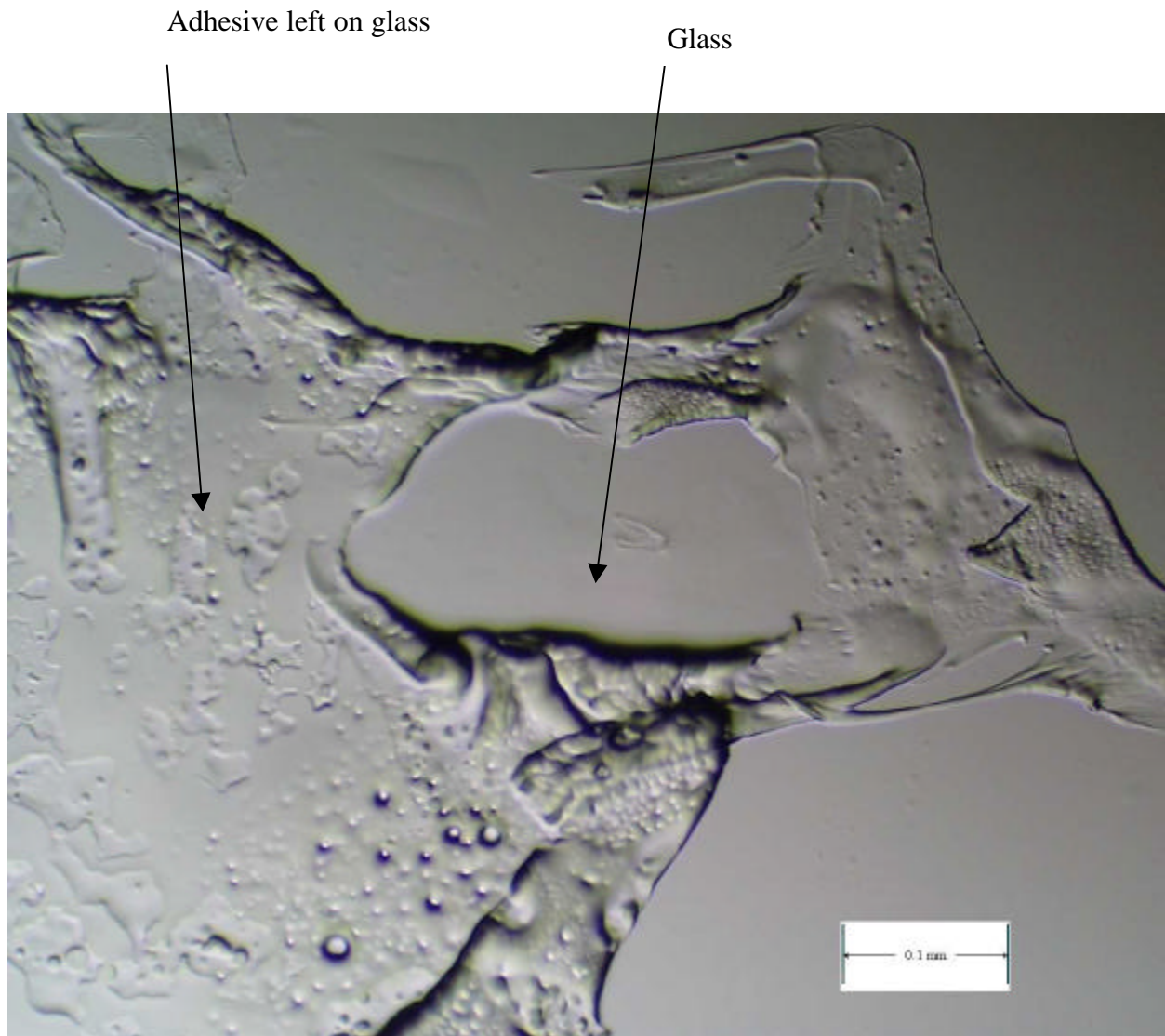


Figure 4.6.4 Optical micrograph of glass slide adherend with traces of adhesive remaining on surface following testing

4.6.3 LAP SHEAR TESTING OF ADHESIVE BONDED BOVINE TISSUE

Lap shear specimens using bovine skin bonded with adhesive formulations C were tested to compare to the adhesive strength values found in the literature for other gelatin based tissue adhesives. The average shear strength of lap joints of bonded bovine (cow) skin was lower than lap joints of bonded glass substrates, likely due to the lower surface tension of cow skin compared to glass, Table 4.6.2. The average shear strength of adhesive formulation C bonded to cow skin is lower than the adhesive strength of gelatin based tissue adhesives reported in the literature but is within one or two orders of magnitude. A comparison to the strength values found in the literature (all units changed to kPa) is given in Table 4.6.3. The measured adhesive strength values found in the literature are variable since they are affected by both the surface properties of the tissue substrate and the joint geometry used. In general, the shear strength of a lap joint is roughly half the strength of a butt joint.⁴⁷ The surface tension of the tissue substrates is variable by tissue type and the wetness of the tissue. It is worth mentioning that extensive efforts to dry the cow skin surface were not made and the methods employed by the various authors are unknown. The wetness of the cow skin may be the cause of lower bond strength values compared to the literature. A fracture energy analysis would serve as a better comparison between bonded tissue joints since the fracture energy is independent of specimen geometry.⁴⁷

Table 4.6.2 Comparison of average shear strength of bovine skin to glass substrate adhesive specimens

	Average Shear Strength (kPa)			
	Glass Substrate			Bovine Skin
	Formulation C	Formulation W	Formulation G	Formulation C
Fresh	23±15	15±5.5	16±5.5	3.6±0.27
Dried	110±12	80±12*	75±24*	

Table 4.6.3 Table of measured adhesive strength of bonded tissue found in the literature with comparison to formulation C bonded to cow skin

Adhesive	Substrate	Test Joint Method	Test time after initial bond	Bond strength (kPa)	Note
GR-Glyoxal Formulation C	Cow skin	Lap shear	1 hr	3.6±0.27	
Gelatin/ Formaldehyde ⁴	Cemented beef tissue plugs	Butt joint	5 min	19±3.2	Ringer's solution
			15 min	39±4.9	
			1 hr	45±5.8	
			18 hr	23±5.9	
GRF ⁴			5 min	26±5.4	Ringer's solution
			15 min	49±5.1	
			1 hr	61±4.9	
			18 hr	91±12	
Polyurethane ⁴			15 min	21±2.9	Ringer's solution
			1 hr	34±3.1	
			18 hr	54±4.9	
Cyanoacrylate ⁴			5 min	7.8±2.2	Ringer's solution
	15 min	12±2.0			
	1 hr	20±3.1			
	18 hr	20±2.9			
Gelatin/ Glutaraldehyde ²⁹	Pig skin	Lap shear	N/A	25	
GRF ⁵²	Pig cartilage	Butt joint	N/A	150	
	Pig bone			200	
	Pig skin			70	
GR-DIAL ⁵²	Pig cartilage			21	
Cyanoacrylate ⁵²	Pig cartilage			1000	
	Pig bone			1400	
	Pig skin	1200			
Fibrin glue ⁵²	Pig cartilage	Lap shear		700	
	Pig cartilage	Butt joint	N/A	4.9	
	Pig bone			11	
	Pig skin			19	
GRFG ⁵³	Sheep thoracic aorta	Butt joint	N/A	13.8±10.0	Wet, 5 N applied
				47.8±17.6	Wet, 20 N applied
				35.0±16.4	Dry, 5 N applied
				170.5±41.5	Dry, 20 N applied

N/A: not available